ANTIOXIDANTS & REDOX SIGNALING
Volume 11, Number 7, 2009

DOI: 10.1089/ars.2008.2348

Comprehensive Invited Review

Redox Control of Protein Conformation in Flavoproteins

Toshiya Senda,[1] Miki Senda,[2] Shigenobu Kimura,[3] and Tetsuo Ishida[4]

Reviewing Editors: David P. Ballou, Kiyoshi Fukui, Alexander Galkin, Peter Macheroux, and Javier Sancho

Abstract

Flavin adenine dinucleotide (FAD) and flavin mononucleotide (FMN) are two flavin prosthetic groups utilized as the redox centers of various proteins. The conformations and chemical properties of these flavins can be affected by their redox states as well as by photoreactions. Thus, proteins containing flavin (flavoproteins) can function not only as redox enzymes, but also as signaling molecules by using the redox- and/or light-dependent

[1]Biomedicinal Information Research Center, National Institute of Advanced Industrial Science and Technology, Tokyo, Japan.
[2]Japan Biological Informatics Consortium, Tokyo, Japan.
[3]Department of Biomolecular Functional Engineering, Ibaraki University, Ibaraki, Japan.
[4]Department of Biochemistry and Molecular Biology, Shiga University of Medical Science, Shiga, Japan.

changes of the flavin. Redox and light-dependent conformational changes of flavoproteins are critical to many biological signaling systems. In this review, we summarize the molecular mechanisms of the redox-dependent conformational changes of flavoproteins and discuss their relationship to signaling functions. The redox-dependent (or light-excited) changes of flavin and neighboring residues in proteins act as molecular "switches" that "turn on" various conformational changes in proteins, and can be classified into five types. On the basis of the present analysis, we recommend future directions in molecular structural research on flavoproteins and related proteins. *Antioxid. Redox Signal.* 11, 1741–1766.

I. Introduction

Flavin adenine dinucleotide (FAD) and flavin mononucleotide (FMN) are the most commonly used flavins as oxidation-reduction (redox) active cofactors in flavoproteins. In addition to their function as cofactors of flavoenzyme, FAD and FMN play important roles in biological signaling, such as blue light-mediated signal transduction and electron transfer reactions. The flavoprotein senses the redox and/or light signal using flavin, and interacts with (or dissociates from) another signaling protein (or domain) to transduce the signal. Several studies have suggested that interactions between signaling flavoproteins and other signaling proteins are frequently regulated by redox-dependent conformational changes of the flavoprotein. Because the conformational changes of flavoproteins are likely to be triggered by the redox-dependent (and/or light-dependent) change of the flavin cofactor, the coupling between the flavin redox chemistry and changes in protein conformation are critical problems in understanding the mechanism of biological signaling by flavoproteins.

The recent development of kinetic crystallography (16) has made it possible to follow the redox-dependent conformational changes of flavoproteins in atomic detail. Spectroscopic analyses in solution have also contributed to reveal conformational and chemical property changes around the flavin. In particular, spectroscopic analyses can probe fast changes around the flavin. These analyses have accumulated structural evidence that the redox-dependent conformational change of flavin induces a conformational change of the *whole* protein, which, in turn, regulates the protein-protein interaction.

In this review, we focus on flavin-containing signaling proteins that show a redox-dependent conformational change. We start with a brief description of the chemical and structural properties of flavin, analyze the interaction between flavin and proteins on the basis of the tertiary structures of the flavoproteins, and categorize the redox-dependent changes occurring around the flavin cofactor in the proteins. Then, various examples of redox-dependent conformational changes of flavoproteins and their functional significance are reviewed. Finally, we propose future directions in this field.

II. Flavin Cofactors

A. Brief history of FMN and FAD

Flavin mononucleotide (riboflavin 5′-phosphate, FMN), which is composed of a 7,8-dimethylisoalloxazine ring with a ribityl phosphate at the N10 atom (Fig. 1A), was first isolated by Theorell (169) in 1935 from yeast old yellow enzyme (181). Old yellow enzyme was the first flavin-containing enzyme (flavoenzyme) to be discovered and has been studied intensively as a model of the flavoenzymes (79). Although some adventitious enzymatic activities of the old yellow enzyme are known, its true physiological substrate and function have long remained elusive. Recently, however, some studies have suggested that in yeast the old yellow enzymes are

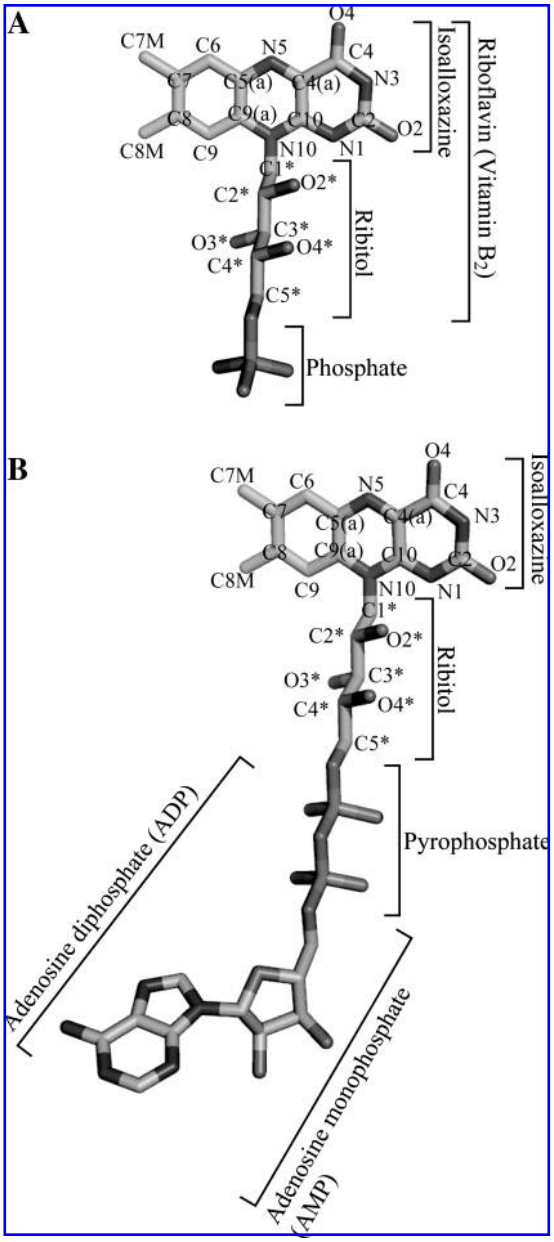

FIG. 1. Structure of flavins. (**A**) Flavin mononucleotide (FMN) and (**B**) flavin adenine dinucleotide (FAD). The atoms in the isoalloxazine ring and ribityl chain are labeled.

placed in the signaling network connecting reactive oxygen species generation, programmed cell death modulation, and cytoskeletal dynamics (56, 127). It is also suggested that plant homologues of the old yellow enzyme are implicated in the metabolism of larger lipid molecules that are made during insect attack (39, 163, 186).

Flavin adenine dinucleotide (riboflavin adenine diphosphate, FAD) was isolated by Warburg and Christian as a cofactor of a D-amino acid oxidase (182). FAD is composed of an isoalloxazine ring with a ribityl chain (riboflavin), and an adenosine diphosphate (ADP) moiety (Fig. 1B). D-Amino acid oxidase catalyzes oxidative degradation of various D-amino acids, including D-serine, to ketoacids, ammonia, and hydrogen peroxide (136). Although the physiological roles of this enzyme in mammals have long been enigmatic, the recent discovery that D-serine plays an important role as coagonist of *N*-methyl-D-aspartate type glutamate receptors (NMDAR) (109, 136) sheds new light on D-amino acid oxidase together with other D-serine-degrading enzymes (166).

B. Redox states of flavins

Flavin can exist in three redox states: oxidized, one-electron-reduced (semiquinone), and fully (two-electron) reduced (hydroquinone) forms (94) (Fig. 2). The spectroscopic properties of flavin in these redox states have been extensively studied and utilized to reveal the reaction mechanisms of flavoenzymes (41, 48, 64, 77, 95, 111, 113, 146). Oxidized FMN and FAD show a specific absorption near 450 nm and exhibit a characteristic yellow color and yellowish green fluorescence. The oxidized isoalloxazine ring has two p*K*a values: ~0 for N1 and ~10 for N3. Therefore, under physiological conditions the oxidized isoalloxazine ring of FAD and FMN is usually in the neutral form as shown in Fig. 2A. When the oxidized flavin is reduced by one electron to the semiquinone form, the specific yellow color turns blue or red, depending on the protonation state of the one-electron-reduced isoalloxazine ring (94, 113) (Fig. 2B). The semiquinone has a p*K*a value of ~8.3 for the N5 atom. The neutral protonated semiquinone is blue (λmax ~560 nm) and the anionic semiquinone is red (λmax 390–410 nm and ~480 nm). Both semiquinone forms are reported for various flavoenzymes. When the isoalloxazine ring is fully reduced to hydroquinone, flavin becomes nearly colorless (it is still pale yellow). Because the hydroquinone has a p*K*a value of ~6.6 for the N1 atom, fully reduced flavin can exist in neutral and anionic forms under physiological conditions (Fig. 2C). It is of note that flavins can be reduced by irradiation of light through intermolecular electron transfer or electron transfer from an external electron donor (photoreduction) (113).

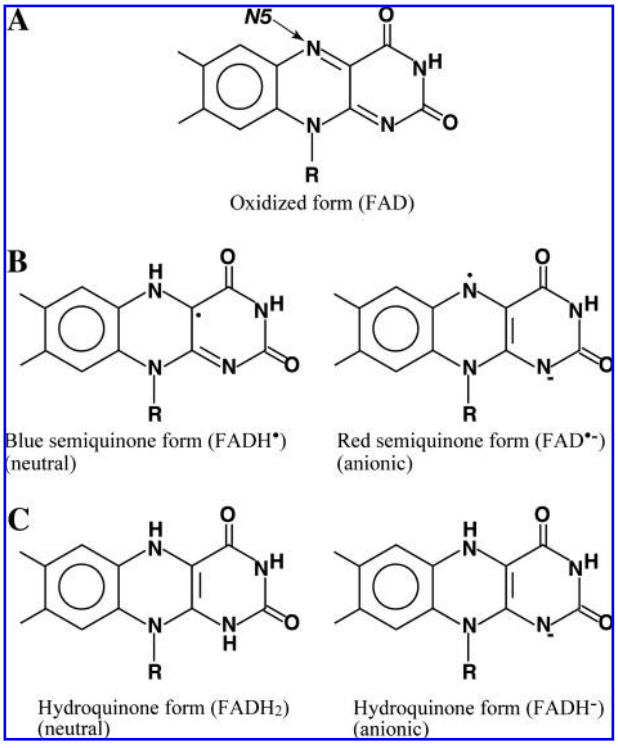

FIG. 2. Redox changes of flavins. (**A**) Oxidized, (**B**) semiquinone (one-electron-reduced), and (**C**) hydroquinone (two-electron-reduced) states of the isoalloxazine ring of flavins (77).

C. Redox-dependent conformational change of the isoalloxazine ring in free flavin

Conformational changes of the isoalloxazine ring of free flavin were analyzed using various flavin derivatives. In the crystal, the isoalloxazine rings of oxidized flavins adopt a planar conformation (42, 90, 171), whereas that of fully reduced flavin adopts a bent conformation along the N5–N10 axis (185). This redox-dependent conformation of the isoalloxazine ring in the crystal might, however, be affected by the crystal packing. Therefore, it cannot be concluded from the crystallographic results alone that in solution the isoalloxazine ring adopts planar and bent conformations in the oxidized and reduced forms, respectively. Several theoretical studies have therefore been performed to examine the conformation of the isoalloxazine ring as a function of redox state. The results obtained by quantum chemical calculations (under vacuum conditions) predict that the isoalloxazine ring in the oxidized state is planar, and that upon two-electron reduction, the isoalloxazine ring is likely to bend along the N5–N10 axis (32, 58, 59, 130, 135, 193). Although the bending angles (15°–25°) reported in these theoretical studies are not identical to each other, theoretical studies support the crystallographic observation that the isoalloxazine ring of fully reduced flavin is bent along the N5–N10 axis (32, 58, 59, 130, 135, 193). The hybridization of N5 and N10 atoms of fully reduced flavin seems to be somewhere between the sp^2 and sp^3 character (193). In the semiquinone form, the isoalloxazine ring was predicted to be very close to planar (193). However, these theoretical results contradicted those obtained by NMR analyses of free flavins in solution.

The NMR analysis of flavin conformation in solution showed that fully reduced flavin in solution contains an almost completely sp^2-hybridized N10 atom, and that the N5 atom also exhibits a predominantly sp^2 character, suggesting that the fully reduced flavin is intrinsically planar in water (121). The energy barrier for the bent-planar transition of the reduced flavin was estimated by NMR as being <4.8 kcal/mol (121). A theoretical calculation also showed that the energy barrier for the bent-planar transition was only ~6.4 kcal/mol (193). The conformation of the isoalloxazine ring therefore seems to be affected by interaction with neighboring molecules.

III. Flavin in the Protein

A. Reactivity of flavins in the protein

Because of the redox properties of the isoalloxazine ring, FAD and FMN can act as redox-active cofactors of flavoproteins that catalyze a wide variety of reactions. In the active site of flavoproteins, the N5 and C4(a) atoms of the isoalloxazine ring have been supposed to be the most reactive with substrates (94). In the oxidized form, the N5 and C4(a) atoms are the most likely targets of nucleophilic attack by substrates. In the reduced states, these two atoms are likely to be subject to an electrophilic attack by substrates. Covalent adducts at the C4(a) atom are frequently found as reaction intermediates (37, 49), consistent with the high reactivity of this atom. In addition to the redox-active chemical nature of the isoalloxazine ring itself, another important determinant in the reaction between the isoalloxazine ring and the substrate is the relative position of the substrate to the isoalloxazine ring in the flavoprotein–substrate complex. Hydrogen bonds between main-chain and/or side-chain atoms of the protein and the flavin N1, N3, O2, and O4 atoms can also affect the reactivity of the isoalloxazine ring.

B. Interaction between flavins and the protein

As of July 2008, there were 726 and 356 entries for FAD- and FMN-containing proteins in the Protein Data Bank (PDB) (13), respectively. First, we analyzed the interaction between the isoalloxazine ring of the protein-bound flavin and the apoprotein moiety (Fig. 3). Interestingly, the isoalloxazine ring of FMN shows a significant preference for interactions with protein side-chain atoms, whereas the isoalloxazine ring of FAD interacts mainly with protein main-chain atoms (Fig. 3A and B). In the case of FAD, the O2, N3, and O4 atoms interact predominantly with main-chain atoms. On the other hand, side- and main-chain atoms contribute similarly to interactions with the O2, N3, and O4 of FMN. Since main-chain atoms are generally less mobile than the side-chain atoms, these results suggest that the isoalloxazine ring of FAD is more tightly fixed to the protein than that of FMN.

As shown in Fig. 3A, the N1 and N5 atoms of the isoalloxazine ring of FAD exhibit a slightly greater tendency than the O2, N3, and O4 atoms to interact with side-chain atoms. These two atoms change their protonation states depending on the redox states of the flavin and the environmental pH (Fig. 2). The change in the protonation states of the N1 and/or N5 atom can induce a rearrangement of the hydrogen bond network around the isoalloxazine ring (see below). Since the side chain is more flexible than the main chain, the interactions of the N1 and N5 atoms with side-chain atoms are likely to be suitable for allowing the rearrangement of the hydrogen bond network. In addition, as shown below, the rearrangement would further lead to conformational changes of the overall structure of the protein.

Next, we analyzed the environment of the isoalloxazine ring using a value indicative of the solvent-accessible surface area. It is frequently used as a quantitative indicator to assess the environment of specific atoms in a macromolecule. Approximately 95% of the isoalloxazine rings of FAD in the flavoproteins deposited in PDB (Fig. 3C) are mostly buried in the protein with <10% of the fractional solvent accessible surface area. This fact suggests that changes occurring in the conformation and/or protonation states of the isoalloxazine ring of FAD would produce a "driving force" from inside of the protein to perturb the protein structure. The isoalloxazine ring of FMN showed the fractional accessible surface area of <10% for ~75% of the FMN-containing proteins as shown in Figure 3D. However, the isoalloxazine ring of the FMN of a significant number of proteins is accessible from outside the protein.

The interactions between the (pyro)phosphate moiety of flavin and the protein also have frequently observed patterns. Analysis of crystal structures of FMN-containing proteins in the PDB showed that, in many cases, the phosphate moiety of FMN is located close to the N-terminal end of the α-helix. The negative charge of the phosphate seems to stabilize the interaction with the dipole moment of the α-helix (104). The oxygen atoms in the phosphate also interact with amide protons of the main chain and positively charged residues, such as Arg.

In the case of FAD, interactions between the pyrophosphate moiety and the protein have also been considered to be predominant factors in stabilizing the FAD binding. Dym and Eisenberg proposed four types of FAD-binding folds (35), each of which possesses a conserved motif to interact with the pyrophosphate. The negative charge of the pyrophosphate interacts with positively charged amino acids, amide protons of the protein main chain, or α-helix dipoles. The adenosine moiety of FAD seems also to stabilize the cofactor binding. Although there are some documented motifs for adenosine-moiety binding, the conservation of these motifs is less strict than those of the pyrophosphate-binding motifs.

C. Conformation of the isoalloxazine ring in the protein

Our comprehensive analysis of the bending angle of the isoalloxazine ring of all the flavoproteins deposited in PDB showed that the calculated bending angles range from 0° to 34° (Fig. 3E and F). The largest bending angle was observed for thioredoxin reductase (34°) (99). The isoalloxazine ring in most flavoproteins shows a bend of <10°, or a nearly planar structure. However, a significant number of flavoproteins contain flavin with bending angles >10°.

Interestingly, some flavoproteins contain oxidized flavin with a bent isoalloxazine ring. For example, monoamine oxidases (15, 108), polyamine oxidase (14), nitroalkane oxidase (125), L-amino acid oxidase (132), and cholesterol oxidase (100) have a bent isoalloxazine ring in their oxidized state. In the case of L-phenylalanine oxidase, the isoalloxazine ring of FAD showed a planar conformation in the crystal of the enzyme with its prosequence, but the removal of the prosequence changed not only the protein conformation but also the bending angle of the isoalloxazine ring (71); the bending angle of the L-phenylalanine oxidase without the prosequence was ~15°. This example suggests that the protein conformation affects the conformation of the isoalloxazine ring (see Section II-C).

The group of Franz Müller performed intensive NMR analyses of isoalloxazine-ring conformations and their interactions with proteins (10, 11, 139, 150, 175–178). This group developed a method to probe the conformations of flavin and its interactions with proteins using ^{13}C and ^{15}N NMR spectroscopy (120–122). They discovered that the hybridization of the N10 and/or N5 atoms changes from an sp^2-like to sp^3-like character upon reduction in the following flavoproteins: riboflavin-binding protein (120), old yellow enzyme (10, 11), *p*-hydroxybenzoate hydroxylase (178), electron-transfer fla-

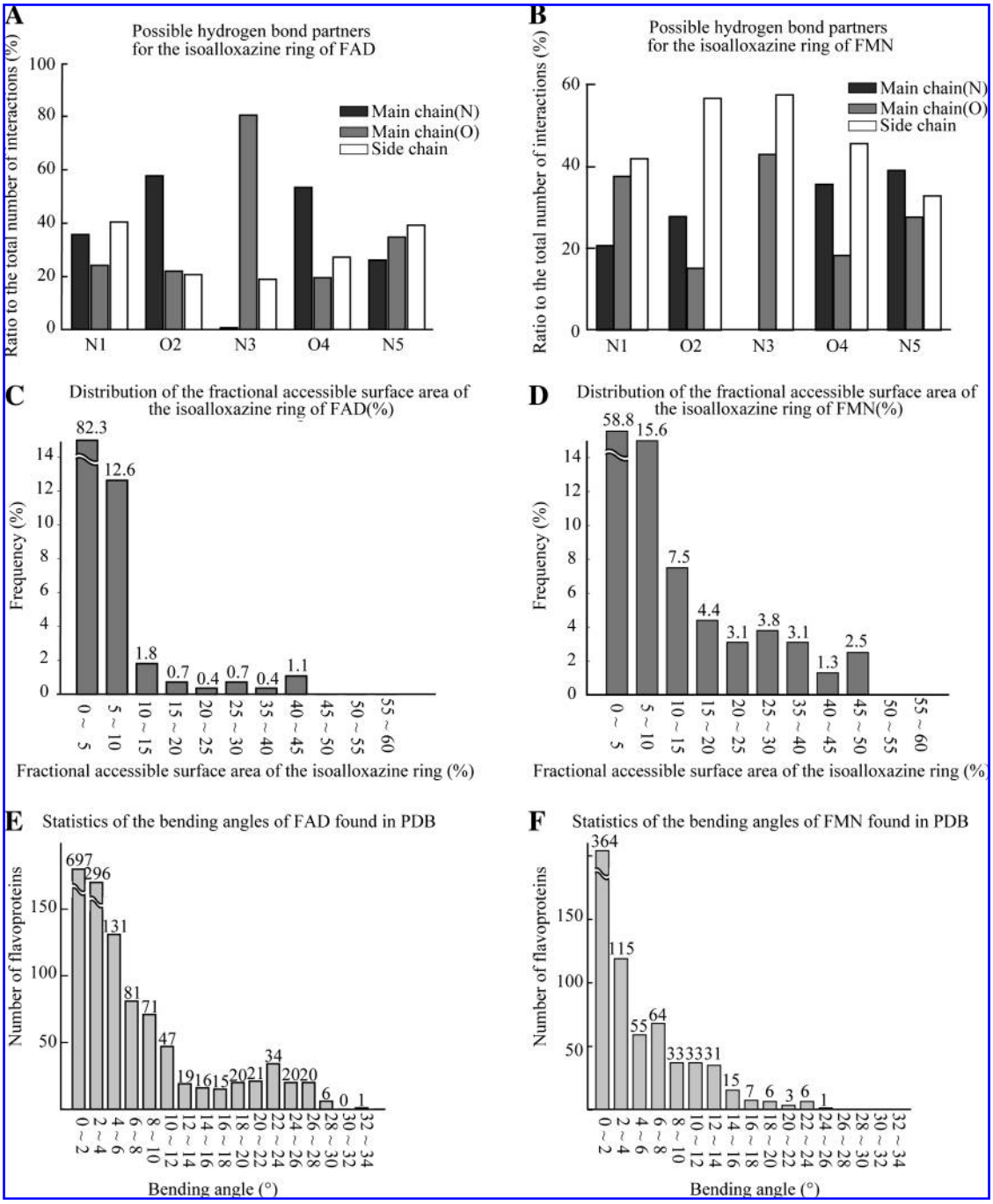

FIG. 3. Analysis of the flavin conformation in the protein. (**A**, **B**) Distribution of protein atoms interacting with the N1, O2, N3, O4, and N5 atoms of the isoalloxazine ring of FAD (**A**) and FMN (**B**). The coordinates were obtained from PDB, and the interactions were analyzed using the program *CONTACT* in the CCP4 suite (28). (**C**, **D**) Distribution of the fractional solvent-accessible surface area of the isoalloxazine ring of FAD (**C**) and FMN (**D**) among all flavoproteins examined. The solvent-accessible surface area was calculated by the algorithm of Lee and Richard (97) using the *SURFACE* program in the CCP4 suite (28). The fractional solvent-accessible surface area of the isoalloxazine ring in the protein was determined by dividing the calculated solvent-accessible surface areas of the protein-bound isoalloxazine ring with that of the isoalloxazine ring of free flavin. (**E**, **F**) Statistics of the bending angle of the isoalloxazine ring of FAD (**E**) and FMN (**F**). When redundant entries were found for a certain flavoprotein in the PDB, only one of them was selected and used for the calculations of **A**–**D**.

voprotein (53), flavocytochrome b_2 (40), and thioredoxin reductase (36). The bends of the isoalloxazine rings of old yellow enzyme (173), *p*-hydroxybenzoate hydroxylase (180), flavocytochrome b_2 (168), and thioredoxin reductase (99) in solution conditions were confirmed by their crystal structures. Several examples of redox-dependent conformational changes of the isoalloxazine ring of flavins were also obtained from X-ray crystallographic studies. For example, thioredoxin reductase (55, 99), mercury reductase (96), Proline utilization A (PutA) (192), and ferredoxin reductase BphA4 (154) showed

redox-dependent conformational changes of the isoalloxazine ring. In some cases, conformational changes of the isoalloxazine ring induce further conformational changes of the protein.

IV. Redox-Dependent Conformational Changes of Flavins and Flavoproteins

A. Flavins as a molecular switch

As described above, FAD and FMN change their conformations and/or protonation patterns according to their redox states and environment. Since these changes of flavin properties alter interactions with protein main/side-chain atoms, the redox-dependent changes of flavins can function as a molecular switch to turn on and off a conformational change of the flavoprotein. Comprehensive analysis of the tertiary structures of flavoproteins in the PDB revealed that there are several flavoproteins that show redox-dependent conformational changes and that the conformational change around the flavin can be categorized into five classes, each of which is considered to be triggered by a distinct "flavin-molecular switch".

B. Bend of the isoalloxazine ring

Some flavoproteins showed not only a redox-dependent change in the bending angle of the isoalloxazine ring, but also a redox-dependent conformational change of the protein, which seems to be induced by the conformational change and possibly the protonation and hydrogen-bonding interactions of the flavin. Mercury reductase (96) and thioredoxin reductase (55, 99) are typical examples. Conformational changes of the isoalloxazine ring seem to cause close contacts of the nearby protein atoms with the bent isoalloxazine ring, and these in turn induce shifts of the neighboring residues. Then, the shifts of the residues trigger a change in the relative orientation of the protein domains (Fig. 4A and B). In the case of mercury reductase, the upper part of the molecule (residues 151–269 and residues 345–456) shows a rigid body rotation of $\sim 1.7^\circ$ against the lower part (Fig. 4A). In bacterial thioredoxin reductase, upon reduction, the NADPH domain rotates by $\sim 8^\circ$ as a nearly rigid body (Fig. 4B). In these two flavoproteins, the isoalloxazine ring is accommodated in the cavity that is located between the domains. Therefore, the conformational change of the isoalloxazine ring can cause the relative dispositional change of the domains. It should be noted that mercury reductase and thioredoxin reductase have a glutathione reductase (GR)-like fold (80), although thioredoxin reductase lacks a C-terminal domain (93).

The change of the bending angle of the isoalloxazine ring, however, does not always induce a significant conformational change of the protein (or domain). Indeed, UDP-galactopyranose mutase (12) and the FAD-binding domains of PutA (the PRODH domain) (98, 192) undergo only small conformational changes, even though the isoalloxazine ring goes from nearly planar in the oxidized state to bent by $14^\circ \sim 18^\circ$ in the reduced state (Fig. 4C and D; Table 1).

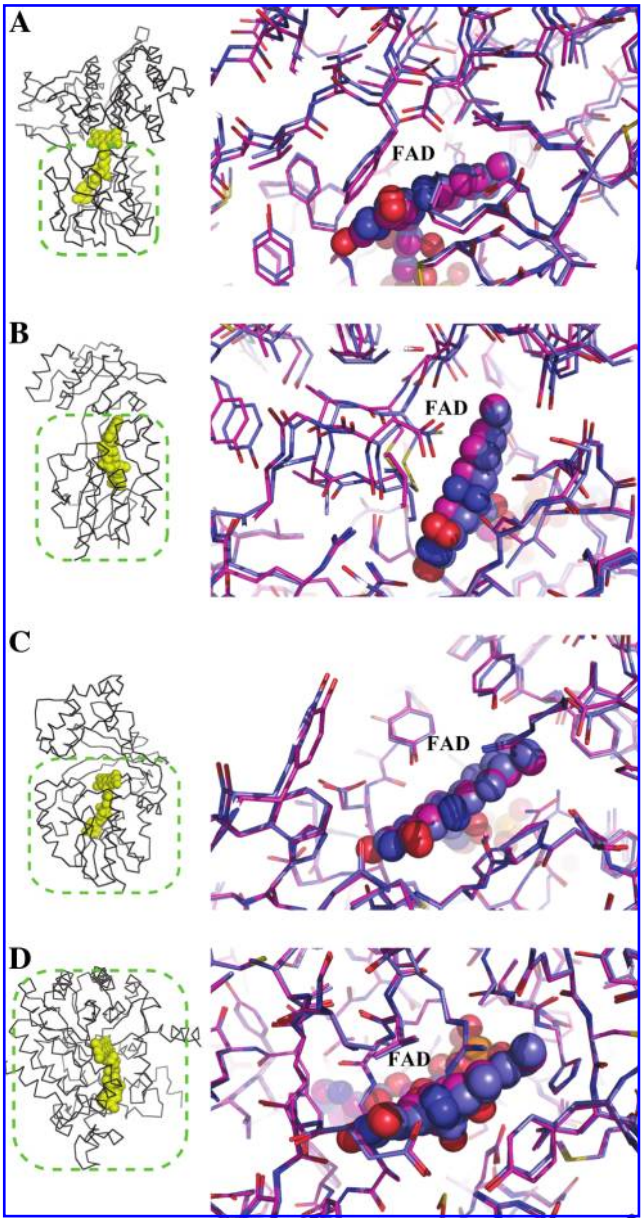

FIG. 4. Conformational changes of proteins induced by the bend of the isoalloxazine ring. (**A**) Mercury reductase (1ZK7, 1ZK9), (**B**) thioredoxin reductase (2Q0K, 2Q0L) (98, 192), (**C**) UDP-galactopyranose mutase (2BI7, 2BI8) (12), and (**D**) PutA (2FZM, 2FZN) (PDB entries used in the figures are given in parentheses). *Left panels* show the overall structures of these proteins (*black*). The Cα atoms enclosed by *green dotted lines* were used for the least-square fittings of these proteins (see Table 1). *Right panels* are close-up views around the isoalloxazine ring of the superposed structures. The least-square fittings were performed using the program *LSQKAB* in CCP4 suite (28). The FADs are shown in sphere models. *Violet and blue structures* represent the proteins with planar and bent isoalloxazine rings, respectively. *Yellow sphere* models in the *left panels* represent the bound FAD.

C. In-out conformational conversion of the isoalloxazine ring

This type of conformational change of FAD was first found in the crystal structure analysis of 4-hydroxybenzoate hydroxylase (44). In the resting state, the flavin is in dynamic equilibrium between an *out* and an *in* state (Fig. 5A). In the *out* state, substrate and product can enter and leave the site where hydroxylation takes place. After binding to the substrate, the isoalloxazine is primarily in the *in* conformation. Upon binding to NADPH, a major conformational change

Table 1. Summary of Least-Square Fittings of FAD-Containing Flavoproteins Between Two Distinct States

Protein	*PDB ID*	*Bending angle (°)*	*Comments*	Cα rmsd (Å) *Superposition using a FAD-binding domain (residue range)*	Cα rmsd (Å) *Superposition using all coordinates (residue range)*
Hg reductase	1ZX9	1.42	PEG form crystal	0.328	0.404
	1ZX7	10.47	Salt form crystal	(4–150*, 270–344)	(4–456*)
PutA	2FZN	2.83	Oxidized form	0.151	0.297
	2FZM	20.97	Reduced form	(261–610)	(88–610)
Thioredoxin reductase	2Q0K	0.40	Oxidized form	0.258	0.906
	2Q0L	22.06	Reduced form	(1–113, 240–310/ chain B)	(1–310/chain B)
UDP-Galactopyranose mutase	2BI7	0.68	Oxidized form	0.179	0.237
	2BI8	14.49	Reduced form	(2–82, 188–249, 315–384)	(2–384)
Vivid	2PD7	0.75	Ground state	0.228	0.356
	2PDR	8.26†	Light excited state	(73–184/ chain A)	(38–184/ chain A)
MICAL	2BRY	0.40	Oxidized form (*out* form)	0.428	0.815
	2C4C	26.4	Reduced form (*in* form)	(7–233, 368–487/ chain A)	(7–487/ chain A)
LOV (PHY3)	1G28	0.65	Ground state	—	0.275
	1JNU	3.00	Light excited state	—	(929–1032/ chain A)
BphA4	2GQW	3.62	Oxidized form	0.221	0.334
	2YVF	14.2	Reduced form	(6–111, 238–317)	(6–406)
BLUF (AppA)	1YRX	0.70	Trp_{in} form	0.864	2.371
	2IYG	0.30	Trp_{out} form	(15–100/ chain A)	(15–130/ chain A)
Flavodoxin	5NLL	3.38	Oxidized form	—	0.244
	5ULL	5.92	Reduced form	—	(1–138)

*Residues 105–110 were deleted for the large discrepancy due to crystal packing.
†The isoalloxazine ring forms a cysteinyl-flavin adduct at the C4(a) atom.
Superpositions were performed using the program *LSQKAB* in the CCP4 suite (28).

occurs in which the isoalloxazine moves to the *out* position where the N5 is exposed to solvent and NADPH can deliver a hydride to reduce the flavin. The newly formed reduced flavin anion is drawn into the electrostatically positive hydroxylating site where the reactions with oxygen and the hydroxylation take place. Then, it is presumed that the enzyme enters an equilibrium between the *in* and *out* conformations to release the product and bind another substrate (38, 180).

It has been revealed that the *in–out* conformational change of FAD can in some cases also induce a conformational change in the protein. When the isoalloxazine ring is accommodated in the cavity located between two domains, the *in–out* conformational conversion of the isoalloxazine ring can affect the relative orientation of the domains. The crystal structure analysis of the MICAL (molecule interacting with CasL) protein in both oxidized and reduced forms revealed that the shift of the isoalloxazine ring from the *out* to the *in* position induces a significant conformational change of the protein (Table 1) (162). The *in–out* conversion of the isoalloxazine ring in MICAL mainly changes the relative disposition of the two domains. This conformational change might have functional significance in biological signaling (162).

D. Conformational change of the ribityl chain

A redox-dependent conformational change in the ribityl chain of FAD was observed in the ferredoxin reductase BphA4 (154) and PutA (192). This conformational change seems to have been induced by the configuration change at the N10 atom of the isoalloxazine ring. The isoalloxazine rings

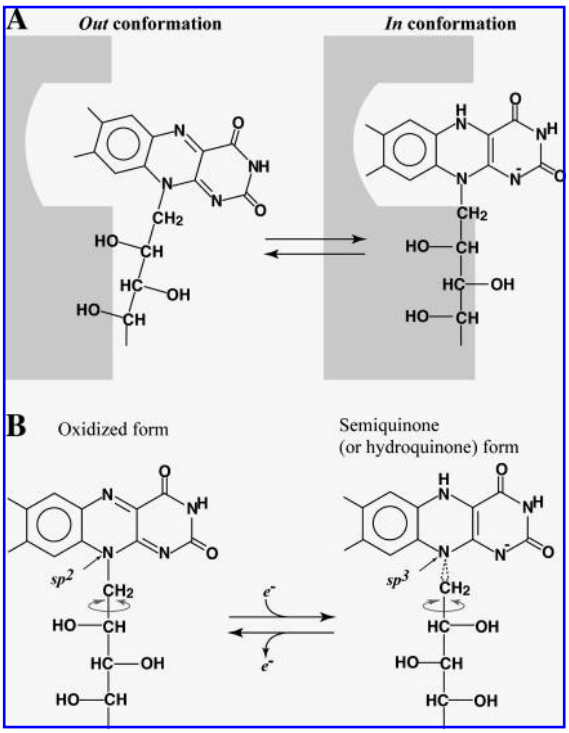

FIG. 5. Classification of the flavin conformational switch (I). (**A**) The transition between the *out* (*left panel*) and *in* (*right panel*) conformations. (**B**) The flip of the ribityl chain associated with the reduction of the isoalloxazine ring.

in BphA4 and PutA are bent upon reduction; the hybridization of the N10 atom was changed from an sp^2 to sp^3 character. The change of the configuration at the N10 atom alters the direction of the bond connecting the N10 atom and the ribityl chain. Because the ADP moiety of FAD is tightly fixed in the protein (see Section III-B), the change of the bond direction would cause an accumulation of mechanical tension in the ribityl chain of FAD. In order to release the accumulated tension, a conformational change occurs in the ribityl chain, which is a highly flexible part of the FAD molecule (Fig. 5B) (154). Since three hydroxyl groups of the ribityl chain usually form hydrogen bonds with protein (and/or solvent) atoms, the conformational change of the ribityl chain would lead to a rearrangement of hydrogen bonds around it. The rearrangement of hydrogen bonds might lead to a conformational change of the protein. Analysis of the crystal structures of PutA showed that the reduction of FAD resulted in changes of the hydrogen bond network around the ribityl chain (see Section V-A). Although no significant conformational change occurs in the FAD-containing domain (the PRODH domain, see Section V-A), the importance of the 2′-OH group of the ribityl chain for the conformational change of the *whole* protein has been biochemically suggested (192).

In the ferredoxin reductase BphA4, the conformational change of the ribityl chain seems also to induce the conformational change of a subdomain (154). The positional shift of the C1* atom of the ribityl chain pushes a part of the subdomain, inducing its conformational change (see Section V-E-2).

E. Changes in interactions with the N5 atom

As described above, the N5 atom is the most frequently involved in the redox reactions of flavins (see Section III-A). The protonation state of the N5 atom changes with the redox state of flavin (Fig. 2). In the oxidized state, the N5 atom does not have a proton (Fig. 2A) and functions as a proton acceptor for hydrogen bonds. Therefore, various kinds of proton donors can form hydrogen bonds with the N5 atom in the oxidized state. On the other hand, fully reduced and one-electron-reduced neutral semiquinone flavins (Fig. 2B and C) have a proton on the N5 atom. In these reduced states, a hydrogen bond acceptor such as a main-chain carbonyl group can make a hydrogen bond with the protonated N5 atom. Due to these properties of the N5 atom, this site can be utilized as a "molecular switch" to sense changes of the redox state of flavins. There are three types of molecular switch involving the N5 atom.

The first type of molecular switch has a hydrogen bond between the N5 atom of the oxidized flavin and a protein atom(s). The hydrogen bond is, however, broken in the fully reduced and neutral semiquinone states, inducing a conformational change of the protein (Fig. 6A). This type of molecular switch was observed in the bacterial ferredoxin reductase BphA4 (154). In this case, Lys53 functions as a sensor of the redox state of the isoalloxazine ring. The hydrogen bond between Lys53 and FAD is broken upon reduction of the FAD (Fig. 6A). This change in hydrogen bonding is likely to induce further conformational changes in BphA4 that are required for BphA4 to form a high-affinity binding site for its redox partner protein, BphA3 (see Section V-E-2) (154).

In the second type of molecular switch, the N5 atom does not form a hydrogen bond with protein atoms in the oxidized form. Upon reduction, a hydrogen bond is formed between the protonated N5 atom and a protein atom(s) (Fig. 6B). This type of molecular switch was observed in flavodoxin (107, 184). In this case, a flip of the peptide bond of the main chain enables the formation of a hydrogen bond between the N5 atom of the reduced isoalloxazine ring and the carbonyl oxygen of the flipped main chain (see Section V-D).

The third type of molecular switch was found in the photoreceptor BLUF (blue-light-using flavin adenine dinucleotide) domains, in which the hydrogen bond network including the N5 atom differs under dark and light conditions. Spectroscopic analysis of the BLUF domain suggested that rearrangement of the hydrogen bonds occurs around the N5 atom in the light-

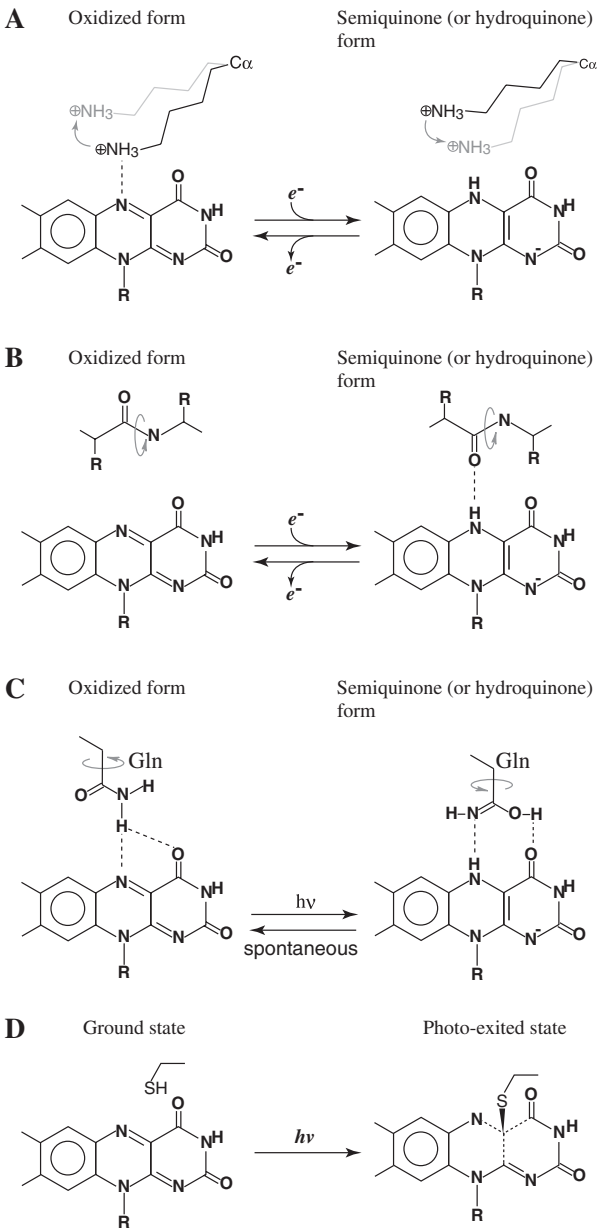

FIG. 6. Classification of the flavin conformational switch (II). (**A**, **B**, **C**) The conformational switches utilizing the N5 atom. Redox-dependent change in the protonation state of the N5 atom is recognized by the neighboring residue. (**D**) Adduct formation at the C4(a) atom.

excited BLUF domain (33, 46, 54, 128). In the ground state (dark state) of the BLUF domain, the amide group of a Gln residue forms a hydrogen bond with the N5 and O4 atoms of the isoalloxazine ring (Fig. 6C, left panel). Upon light activation, a transient change of the protonation state of the N5 atom of the flavin occurs, inducing a hydrogen bond rearrangement between the isoalloxazine ring and the Gln residue to produce a light form. In this process, the Gln residue undergoes a conformational change (Fig. 6C, right panel). Although spectroscopic studies proposed some distinct models for this change, all models proposed that the conformational change of the Gln residue is relevant to further conformational changes in the BLUF domain (see Section V-C-2).

F. C4(a)-adduct formation

This switch utilizes a chemical reaction occurring at the C4(a) atom of the isoalloxazine ring (Fig. 6D); the C4(a) adduct formation is known to trigger several photoreceptors (see Section III-A). The light-excited oxidized flavin forms a covalent adduct between the thiol group of a Cys residue and the C4(a) atom of the flavin (30). The formation of the covalent linkage induces conformational changes of the protein. In addition, the formation of a covalent bond may change the dynamic properties of the protein. This type of conformational change was extensively studied by kinetic crystallography of photoreceptors of the LOV family (30, 198). Crystal structure analyses revealed the detailed process of the cysteinyl-flavin-adduct formation (see Section V-C-1).

V. Redox Control of the Flavoprotein Conformation and Its Biological Functions

A. Proline utilization A (PutA)

In eukaryotes, proline is metabolized to glutamate in mitochondria by two mono-functional proteins, FAD-containing proline dehydrogenase (PRODH) and NAD^+-dependent Δ^1-pyrroline-5-carboxylate dehydrogenase (P5CDH) (134). On the other hand, in some bacteria such as *Escherichia coli* and *Salmonella typhimurium*, a multifunctional flavoprotein, PutA, catalyzes this two-step oxidation of proline to glutamate at the inner cytoplasmic membrane (117, 141, 151). PutA contains a DNA-binding domain (DBD) at the N-terminal portion in addition to the PRODH and P5CDH domains (Fig. 7A) (118). When the available proline levels are low, PutA binds to operator sites and represses the transcription of the proline utilization (*put*) genes *putA* and *putP* (129). The mechanism of the functional switching of PutA from a cytosolic repressor to a membrane-bound dual-functional enzyme has attracted considerable attention.

Earlier enzymatic studies on PutA demonstrated that FAD is required only for PRODH activity and that P5CDH activity requires NAD^+ instead (118). Further studies suggested that the redox state of FAD in the PRODH domain determines the cellular localization of the PutA protein, which controls the PutA function in the cell; the reduced PutA protein is preferentially localized at the membrane (187). When the cellular proline concentration is relatively high, the PRODH domain of PutA is fully reduced through reaction with proline (118) and moves to the membrane to further catalyze the oxidation of proline (Fig. 7B). Electrons in the reduced PutA are transferred to an electron-transfer system of the respiratory chain (117, 151), and the PutA protein returns to the oxidized form to enter the next reaction cycle. When the proline concentration is low in the cell, most PutA proteins are in the oxidized form due to the lack of the substrate proline. Since oxidized PutA has low affinity to the membrane, PutA moves to cytosol and binds to operators for the *put* genes to repress their expression (Fig. 7B). This redox-dependent localization of the PutA protein is consistent with its physiological function.

The linkage between the redox state of FAD and the conformation of the whole PutA molecule was first demonstrated by biochemical experiments. A chymotrypsin digestion study suggested that the redox state of FAD controls the conformation of PutA (19, 194), and that this redox-dependent conformational change is reversible. Thus, it is reasonable to predict that the redox-dependent conformational change of PutA controls the localization of the flavoprotein in the cell.

In order to reveal the redox-dependent conformational change of PutA in atomic detail, several crystal structure analyses of the recombinant PRODH domain of PutA have been performed. The first crystal structure of the PRODH domain was reported in 2003 (98) (Fig. 7C). The PRODH domain forms a dimer in the crystal, each half of which is composed of three structurally distinct domains I, II, and III. Domain III adopts a $\beta_8\alpha_8$-barrel fold that binds oxidized FAD at the C-terminal ends of the β-strands of the barrel. The N5 atom of the isoalloxazine ring and the 2′-OH group of the ribityl chain form hydrogen bonds with Arg431 and Arg556, respectively (Fig. 7D). The crystal structure of the reduced-form PRODHO domain was revealed in 2007 by the same group (192). As shown in Fig. 7E, the reduced FAD shows a bend of the isoalloxazine ring by $\sim 20^\circ$ along the N5–N10 axis (Table 1). This bend seems to induce a "crankshaft" rotation of the upper part of the ribityl chain (192) (Fig. 7E). Because of this conformational change, rearrangements of the hydrogen bonds around the ribityl chain occur. Upon reduction, the hydrogen bond between the 2′-OH group and Arg556 is lost due to the crankshaft rotation of the ribityl chain, and the 2′-OH group forms a new hydrogen bond with the main-chain nitrogen of Gly435 (Fig. 7D). Structure-based biochemical experiments showed that the 2′-OH group, Arg556, and Arg431 were all critical for the redox-dependent affinity of PutA for the lipid vesicles (192). However, a structural comparison between the oxidized and reduced PRODH domains of PutA did not show any significant conformational change of the PRODH domain (Fig. 4D, Table 1). The least-squares fittings of all Cα atoms in the PRODH domain resulted in a root-mean square value of 0.297 Å (Table 1) (98, 192). Since the membrane-binding sites of PutA are suggested to be mainly located in regions C-terminal to the PRODH domain (Fig. 7A) (103, 194), certain redox-dependent conformational changes in the PRODH domain should be propagated to these regions in order to rearrange the membrane-binding sites into the position where it can access the membrane. Because the conformational change in the PRODH domain responsible for the domain rearrangement of the whole PutA protein is unrecognizably small, the redox-induced effect on the PRODH domain should be amplified in a certain mechanism to control the localization of the PutA protein (192). Further analysis of the whole PutA protein with the membrane-binding regions intact will be necessary to reveal the underlying mechanism of the redox-dependent conformational change that is responsible for the redox-dependent localization of this protein.

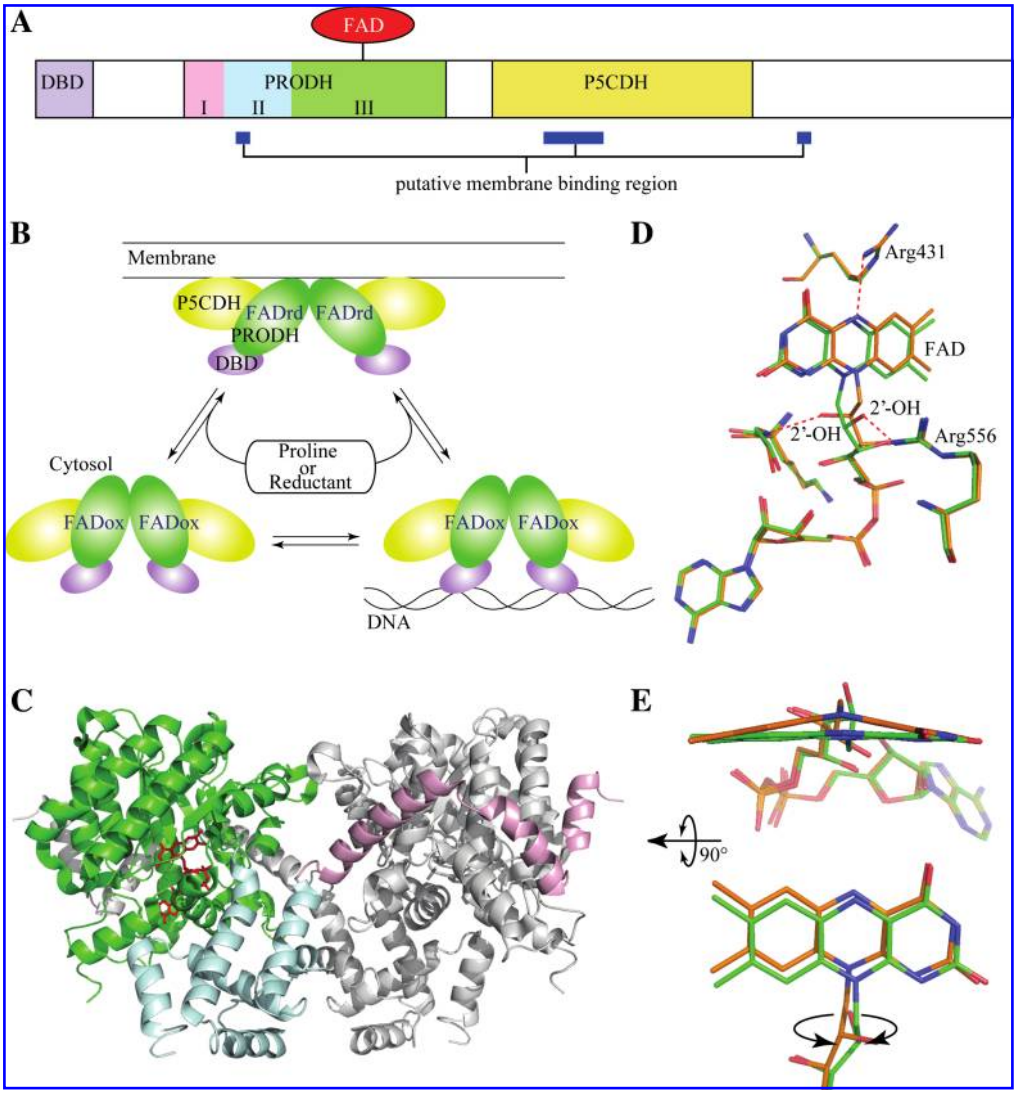

FIG. 7. The PutA protein. (**A**) A schematic view of the primary structure of PutA. Three functional domains, the DNA-binding domain (DBD), PRODH domain, and P5CDH domain, are indicated with distinct colors. Putative membrane-binding regions are shown with *blue bars* below. (**B**) Redox-dependent localization of the PutA protein. The reduced PutA is localized on the membrane. The oxidized PutA binds the *put* gene to repress its transcription. (**C**) Overall structure of the PRODH dimer. Domains I, II, and III (in the left subunit of PRODH) are shown in *pink, cyan*, and *green*, respectively. The right subunit is shown in *light gray*. (**D**) The hydrogen bond network around FAD. (**E**) Redox-dependent conformational change of the isoalloxazine ring of FAD in PutA. *Green* and *orange* molecules in (**D**) and (**E**) correspond to oxidized and reduced forms, respectively.

B. Apoptosis-inducing factor (AIF)

Mitochondrial apoptosis-inducing factor (AIF) was first identified by Susin *et al*. in 1999 (164). AIF has primary structural similarity to bacterial NADH-dependent ferredoxin reductases (157, 164) (Fig. 8A, see also Fig. 14A). Indeed, the crystal structures of human and murine AIFs (116, 190) showed that AIF adopts a folding pattern similar to those of bacterial ferredoxin NADH reductases such as BphA4 and putidaredoxin reductase (157) (Fig. 8B). AIF is composed of three domains, an FAD-binding, an NADH-binding, and a C-terminal domain. The ADP moiety of FAD interacts intensively with the FAD-binding domain. The isoalloxazine ring of FAD is surrounded by all three domains, and each of these domains interacts with the isoalloxazine ring.

AIF is normally localized in the intermembrane space of mitochondria, but its translocation to the nucleus under apoptotic stimulus induces the apoptosis of the cell. Interestingly, Susin *et al*. showed that the apoptosis-inducing activity of AIF was independent of FAD by addition of recombinant AIF lacking FAD to isolated nuclei of HeLa cells and its microinjection into the cytoplasm (164); any putative oxidoreductase activity of AIF is unnecessary for its apoptogenic function under these conditions. The significance of AIF's redox-activity in the apoptogenic function was therefore enigmatic.

Still, the accumulation of biochemical and biological evidence has shed light on the redox-relevant biological activity of AIF. AIF is involved not only in cell death but also in cell survival (119, 137). Some AIF-deficient mouse models have

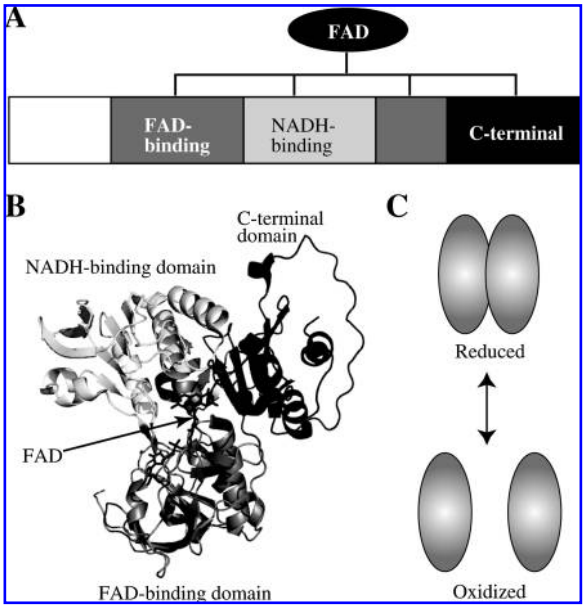

FIG. 8. Apoptosis-inducing factor (AIF). (**A**) A schematic view of the primary structure of AIF. (**B**) The overall structure of AIF, which is composed of three domains: FAD-binding (*dark gray*), NADH-binding (*light gray*), and C-terminal (*black*) domains. (**C**) AIF changes its oligomeric state in a redox-dependent manner.

suggested that mitochondrial AIF is required for maintaining normal mitochondrial functions such as oxidative phosphorylation and energy generation (137). Recently, Sevrioukova's group proposed that the redox-dependent conformational change of AIF is relevant to its biological signaling function, providing new insight into the mechanism by which AIF functions (27), although the details of the molecular mechanism of the redox-dependent conformational changes remain elusive due to lack of the tertiary structural information of the reduced-form AIF.

The Sevrioukova group showed that recombinant AIF forms a dimer upon reduction with NAD(P)H, whereas the oxidized AIF exists as a monomer (27) (Fig. 8C). In the fully reduced AIF, FAD forms a charge-transfer complex (112) with $NAD(P)^+$. Unlike the similar charge transfer complex of BphA4, the reduced AIF is unusually stable even under aerobic conditions. In their study, protease digestion and CD spectroscopy of AIF showed that AIF undergoes redox-dependent conformational changes. It also confirmed that the redox-dependent conformational changes and dimerization observed in recombinant AIF also occurs in the native mitochondrial AIF (27). More importantly, the Sevrioukova group found that NAD(P)H inhibits the release of AIF from the mitochondria. These results suggested that AIF functions as a redox sensor through redox-dependent tertiary and quaternary structural changes.

On the basis of these biochemical analyses, the Sevrioukova group proposed the possible function of AIF as follows (27): When dimeric reduced AIF in mitochondria senses oxidative stress, the membrane-anchored AIF is released by protease activation. AIF translocates to the cytosol and then to the nucleus. In the nucleus, the AIF induces apoptosis through interactions with DNA, when the AIF is in a monomeric form. The group suggested that AIF has dual functions, namely a redox-sensing function with FAD and an apoptosis-inducing function that occurs through interactions with DNA and does not require FAD. Biological analysis with further crystallographic analyses of AIF in various redox states would reveal the mechanism of the monomer-dimer conversion as well as further functional implications of AIF.

C. Photoreceptors

There are three well-known flavin-containing photoreceptor families, light-oxygen-voltage (LOV) domain-containing proteins (18), blue-light-using flavin adenine dinucleotide (BLUF)-containing proteins (50), and cryptochromes (CRY) (138). All these families are blue light receptors, and the mechanism of biological signal transduction mediated by flavin excitation has been investigated in them. Of the three families, intensive analyses of the LOV and BLUF domains have been carried out to reveal the connection between the FAD chemical properties and the conformation of the protein.

1. LOV domain. The LOV domain (18) contains noncovalently bound FMN and belongs to a subset of the Per-ARNT-Sim (PAS) domain superfamily (167, 195) that is utilized by cells to convert input stimuli into signals by regulating protein–protein interactions. The LOV1 and LOV2 domains were first identified as repeating domains in plant phototropin 1 (phot1 or NPH1 (nonphototropic hypocotyl 1)) (Fig. 9A) (25, 26, 68). A phototropin NPH1 that contains a protein kinase domain as well as the two LOV domains (Fig. 9A) is a photoreceptor for phototropism, chloroplast relocation, and stomatal opening of plants (25, 73, 76, 84, 145). The FMN-containing LOV domains of NPH1 act as blue-light receptors (26). Blue light is likely to induce autophosphorylation of the kinase domain of the phototropin by activating the LOV domains. Biochemical and spectroscopic analyses have revealed that a cysteinyl-flavin adduct is formed in the LOV domains by blue light (147, 165).

In order to understand the molecular mechanism(s) of light-induced signaling in plants, crystal structural analyses of LOV domains were performed. The first crystal structure of the LOV domain was reported in 2001 (Fig. 9B) (29), and the light-excited structure of the LOV domain appeared in the following year (30). These crystal structures clearly showed that the light-excited FMN in the LOV domain forms a cysteinyl-flavin covalent adduct as expected from the spectroscopic studies.

Figure 9B shows the crystal structures of the dark-state LOV2 domain derived from *Adiantum capillus-veneris* (29). The LOV2 domain adopts a typical fold of the PAS domain such as that seen in FixL (51). The isoalloxazine ring of FMN is buried inside the LOV2 domain. A cysteine residue, Cys966, which is essential to the light activation of the LOV2 domain, is located above the *si* side of the isoalloxazine ring, and its Sγ atom is $\sim$3.5 Å apart from the C4(a) atom of the isoalloxazine ring (Fig. 9C, upper panel). In the light-excited state, Cys966 forms a cysteinyl-flavin adduct (Fig. 9C, lower panel) (30). This adduct formation results in a deformation of the isoalloxazine ring; the C4(a) atom adopts a tetrahedral configuration. An $\sim 8^\circ$ tilt of the isoalloxazine ring was also observed in the light-excited state (30). Although the side chains of Asn1008, Gln1029, and Phe1010 showed small

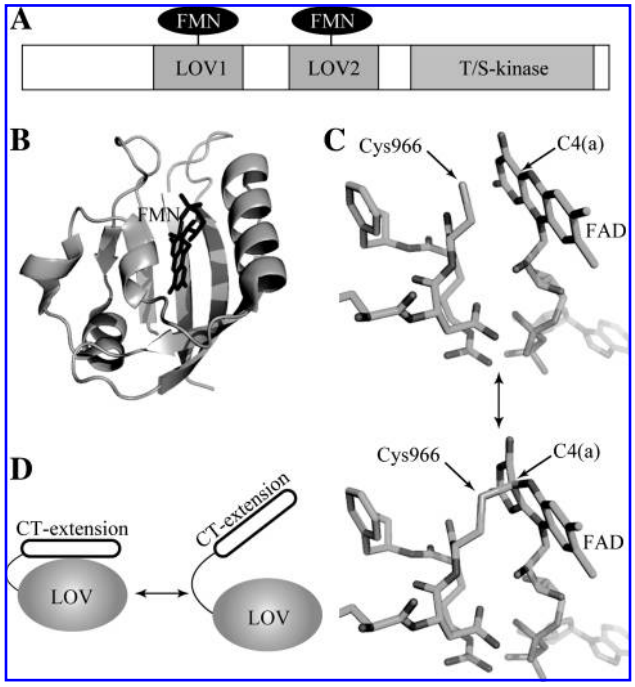

FIG. 9. The LOV domain. (**A**) A schematic view of the primary structure of the LOV domain containing Nph1. Nph1 contains two LOV domains in the molecule. (**B**) Overall structure of the LOV domain. (**C**) Formation of the cysteinyl-flavin adduct in the LOV domain. The *upper panel* shows the ground state, and the *lower panel* shows the light-excited state, in which a cysteinyl-flavin adduct is formed. (**D**) The effect of adduct formation in the LOV domain. The C-terminal extension dissociated from the LOV domain upon light excitation.

conformational changes, no significant conformational changes were observed in the overall structure of the LOV domain (30). The root-mean square value of the LOV domain (PHY3 LOV2) from the least-square fittings was 0.275 Å (Table 1) (29, 30). This value is comparable to or less than the estimated coordinate errors of these crystal structures. Despite the small or undetectable level of structural change in the isoalloxazine ring-containing domain, biochemical analysis suggested that the relationship between the domains seems to be significantly changed in phototropins Nph1. Although crystallographic analysis of the LOV domain core revealed the light-activated structure of the LOV domain, these structures provided no clues to the light regulation mechanism of the kinase domain in Nph1. It remains to be elucidated how local conformational changes in the LOV domain are propagated to the kinase domain in the protein.

One clue regarding this question was initially provided by the NMR analysis of the LOV2 domain with a 40-amino acid C-terminal extension (62). Approximately 20 residues in the extension adopt an α-helix, and the α-helix associates with the LOV domain in the dark state. In the light state, light-induced changes in the LOV domain disrupt the interaction between the C-terminal helix and the LOV domain. This light-dependent interaction between the C-terminal extension and the LOV domain seems to connect the cysteinyl-flavin adduct formation and the kinase activation (Fig. 9D). Indeed, when the Cys residue was replaced with Ser, the disruption of the association of the C-terminal extension with the LOV domain could not be observed by light excitation (62).

Crystallographic analysis of another LOV domain, the LOV domain in Vivid (65), also showed the importance of the extension region (198). In the case of Vivid, the formation of the cysteinyl-flavin adduct induces significant conformational changes in the N-terminal extension region (N-terminal cap). How are the conformational changes in the LOV domain of Vivid utilized for signal transduction? It has been thought that the dimerization of the LOV domain would occur upon light-dependent formation of cysteinyl-flavin adduct (148), because PAS domains are known to act as dimerization domains (69, 70). A recent study on Vivid using size-exclusion chromatography, equilibrium ultracentrifugation, and static and dynamic light scattering suggested that the conformational changes occurring at FMN are propagated in the protein and cause the formation of a rapidly exchanging Vivid dimer (197). The ability to form the dimer is dependent on the length of the N-terminal cap region of Vivid, which showed a significant conformational change in the crystal structure analysis (198). Further structure-based analysis will reveal the complete mechanism of the dimer formation of Vivid and other flavin-containing LOV-family proteins.

Recently, the 1.04 Å-resolution crystal structure of a redox-sensing LOV domain, NifL, was determined (81). NifL is a flavoprotein belonging to the LOV family and modulates transcriptional activation of nitrogen-fixation genes as a redox-sensitive switch (66). The crystal structure of NifL showed that it adopts the characteristic α/β PAS domain fold and binds one FAD molecule (81). Although the fold of the protein is similar to the photoreceptor's LOV domain, residues around the isoalloxazine ring are somewhat different. First of all, Glu70 is located at the corresponding position of the Cys residue that forms an adduct with flavin in the photoreceptor. In addition, there are two water molecules in an isolated cavity inside the molecule, which is located adjacent to the isoalloxazine ring. These water molecules take part in the hydrogen bond network involving the isoalloxazine ring and Glu70, and are thought to have a functional role (81). Although details of the O_2-sensing mechanism remain elusive, the crystal structure suggested that an O_2 molecule reacts with the C4(a) atom of the isoalloxazine ring, and the resultant conformational change would be propagated as found in other LOV-family photoreceptors.

2. BLUF domain. The BLUF (blue-light-using FAD) domain is a blue-light receptor containing FAD as a photosensor (50). Two proteins with BLUF domains were identified in 2002. One is AppA (activation of photopigment and *puc* expression) from *Rhodobacter sphaeroides* (Fig. 10A) (114) and the other is PAC (photoactivated adenylyl cyclase) from *Euglena gracilis* (72). Further studies have isolated other BLUF proteins, such as YcgF from *E. coli* (140) and Slr1694/TII0078 from *Synechocystis* sp. PCC6803 and *Thermosynechococcus elongates* BP-1 (115).

AppA is a transcription factor that controls both redox- and blue light-dependent repression of a photosystem gene expression through control of the DNA-binding activity of the transcription repressor PpsR (133). AppA forms an anti-repressor complex with PpsR in the dark state (the AppA–$PpsR_2$ complex). When AppA is excited by blue light, AppA dissociates from $PpsR_2$. The resulting free $PpsR_2$ binds to DNA to

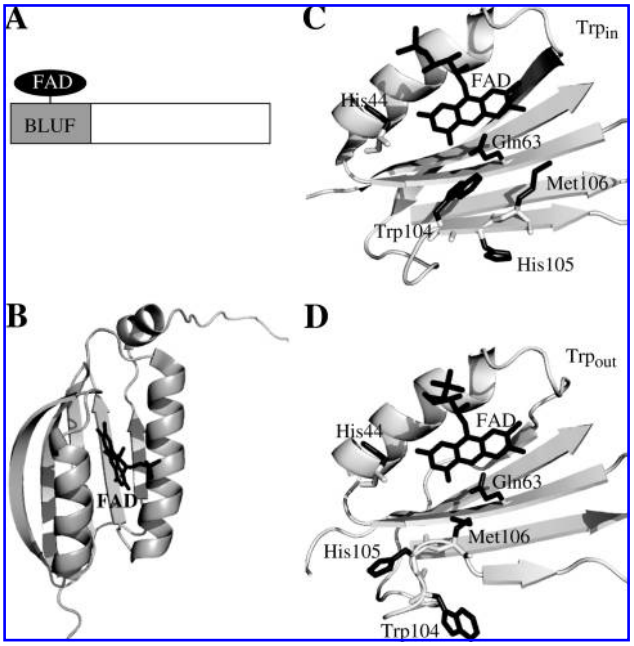

FIG. 10. The BLUF domain. (**A**) A schematic view of the primary structure of AppA containing a BLUF domain. (**B**) Crystal structure of the BLUF domain. (**C**, **D**) Two distinct conformations of Trp_{in} (**C**) and Trp_{out} (**D**).

repress the expression of photosystem genes. Biochemical and biological analyses of the AppA BLUF domain have suggested that the BLUF domain contains FAD to sense blue light (114). The BLUF domain seems to interact with the C-terminal part of AppA in the dark state to cover the binding site for $PpsR_2$. The light-excited BLUF domain is likely to be dissociated from the C-terminal part, facilitating the repression of the photosystem genes (114).

The BLUF domain is composed of ~100 amino acid residues and contains one FAD (Fig. 10A). Spectroscopic analyses of the BLUF domains showed that photoreactions of these domains are reversible cyclic reactions, as are those of other photoreceptors such as the LOV domain (114). The light-excited BLUF domain of AppA showed a significant red shift (~10 nm) in the absorption spectrum, which is a common characteristic of the BLUF domain (114). The light-excited species of the AppA BLUF domain is quite long-lived, decaying back to the resting state in the dark over a 30-min timescale. Each of the BLUF domains exhibits a specific decay time ranging from a few seconds to >30 min. A transient spectroscopic analysis of the Slr BLUF domain suggested that a light-excited species seems to be formed by means of a radical-pair mechanism involving electron and proton transfer from the protein to the FAD (47). The interaction between the isoalloxazine ring and surrounding amino acid residues of the BLUF domain in the light-excited state is likely to be different from that in the resting dark state (Fig. 6C) (63, 115, 172). The mechanism of the photo-signal conversion of the BLUF domain seems to be distinct from that of the LOV domain, in which a cysteinyl-flavin adduct is formed in the photo-excited state.

The crystal structures of the BLUF domain were first reported in 2005 (4, 74, 85). As shown in Fig. 10B, the BLUF domain can be categorized as an $\alpha + \beta$ sandwich fold with two long α-helices located on one side of the five-stranded β-sheet. The other side of the β-sheet is utilized for the dimerization. The fold of the BLUF domain is similar to that of [4Fe–4S] ferredoxins. The isoalloxazine ring of FAD is sandwiched by two α-helices, and the adenine moiety is exposed to the solvent, whose electron density was invisible. The binding pocket for the isoalloxazine ring is lined by conserved amino acid residues in the BLUF-family proteins. The crystal structure of the AppA BLUF domain showed that the conserved Gln63 interacts with the N5 atom of the FAD (Fig. 10C and D).

A series of crystallographic analyses of BLUF domains of AppA from *R. sphaeroides* and Slr1694 from *Synechocystis* sp. PCC6803 revealed that the conserved Trp residue (Trp104 in AppA, Trp91 in Slr1694) adopts two distinct conformations, Trp_{in} and Trp_{out} (Fig. 10C and D) (4, 74, 75, 191). Spectroscopic analyses suggested that the photoexcited isoalloxazine ring triggers a rearrangement of the hydrogen bond network, in which Gln63 interacting with the N5 atom plays an important role in AppA (Gln50 in Slr1694) (see Section IV-E). Several models have been proposed to explain the conformational change of the conserved Gln residue. In these models, the conformation and hydrogen bond(s) of the conserved Gln residue change in response to the transient protonation state of the N5 atom of the light-excited FAD. Despite the differences among these models, in all of them, a conformational change in Gln63 (Gln50 in Slr1694) is believed to induce the conformational change of Met106 (Met93 in Slr1694), leading to significant change in Trp104 (Trp91 in Slr1694). These changes also induce a conformational change of the main chain (Fig. 10C and D). Since the light-excited BLUF domain spontaneously returns to the dark state within a timescale of seconds or minutes, the light-excited state seems not to be an energetically stable form. Most probably, the light-excited state of the BLUF domain is a meta-stable state.

There is debate on the assignment of the Trp_{in} and Trp_{out} conformations to the functional states of the photocycle of the BLUF domain. The first group assigned the Trp_{in} conformation to the dark state on the basis of their analysis of the fluorescence of the conserved Trp residue (75). They concluded that the environment of the Trp residue changed from a hydrophobic one in the dark state to a more hydrophilic one in the light-excited state. The other group, however, assigned the Trp_{in} and Trp_{out} conformations to light-excited and dark state, respectively, judging from the calculated electronic transition energies and vibrational frequencies of the proposed dark and light states. Their theoretical results are consistent with the optical and IR spectral changes observed during the photocycle (33).

Detailed analyses of the local structure around the isoalloxazine ring of FAD showed some changes in the BLUF domain that are possibly linked to conformational changes of the whole AppA molecule in the photocycles, if the conformational change of the whole molecule is congruent to that of the BLUF domain. The structural analysis of the BLUF domain with C-terminal part of AppA will reveal how the conformational changes induced in the BLUF domain by light-excitation control the function of AppA.

3. Cryptochrome (CRY). Cryptochrome (102), a blue-light photoreceptor, was discovered in 1993 as a regulator of hypocotyl elongation in *Arabidopsis thaliana* (1). Biochemical analysis of this cryptochrome (referred as CRY1) showed that

CRY1 is a FAD-containing flavoprotein and that the FAD in CRY1 can be photoreduced to produce the neutral semiquinone form under anaerobic conditions (101). Cryptochromes were also found in mammalian cells. Reverse genetic and biochemical studies indicated that mammalian cryptochromes play a critical role in circadian rhythms (89, 170, 174). Mammalian cryptochrome seems to be a circadian photoreceptor that synchronizes circadian rhythms with light-dark cycles (photoentrainment). However, further investigations are necessary to establish the role of photoreception in mammalian cryptochromes.

Intriguingly, cryptochromes show sequence homology to DNA photolyases that catalyze light-dependent DNA-repairing reactions (Fig. 11A) (1, 101). Despite the sequence homology between them, cryptochromes have no detectable photolyase activity. Cryptochromes differ from photolyases by a characteristic C-terminal domain. Biological and biochemical analyses in *Drosophila* and *Arabidopsis* have revealed that the C-terminal domain of cryptochromes regulates the interaction of cryptochromes with circadian transcription factors (22, 31, 143, 161, 179, 188, 189). However, the relationship between the light detection of FAD in the cryptochrome and possible conformational changes of the C-terminal domain are still not well understood and should be addressed in future research.

The first crystal structure of a cryptochrome-family protein, cryptochrome DASH derived from *Synechocystis* sp., was reported in 2003 (Fig. 11B) (20). Cryptochrome DASH resembled DNA photolyases in three-dimensional structure, as expected from the sequence homology between them. Cryptochrome DASH is composed of two domains, the α/β and α domains. The two domains are linked by a connecter region (domain). The bound FAD adopts a U-shaped conformation and is located deep inside the α domain. It should be noted that this cryptochrome lacks the C-terminal domain in contrast to most cryptochromes such as CRY1. The crystal structure of CRY1 was determined as the C-terminal truncated form in 2004 (17). The C-terminal domain of CRY1 was thought to be an unstructured region; this was confirmed by NMR spectroscopy (131). A partial digestion study using proteases suggested that a light-dependent conformational change occurs in the CRY1 C-terminal domain. However, the light-induced change around the FAD remains elusive in cryptochromes (131). Analysis of the conformational changes around the FAD would lead to a better understanding of the molecular mechanisms of the light-induced change in the C-terminal domain.

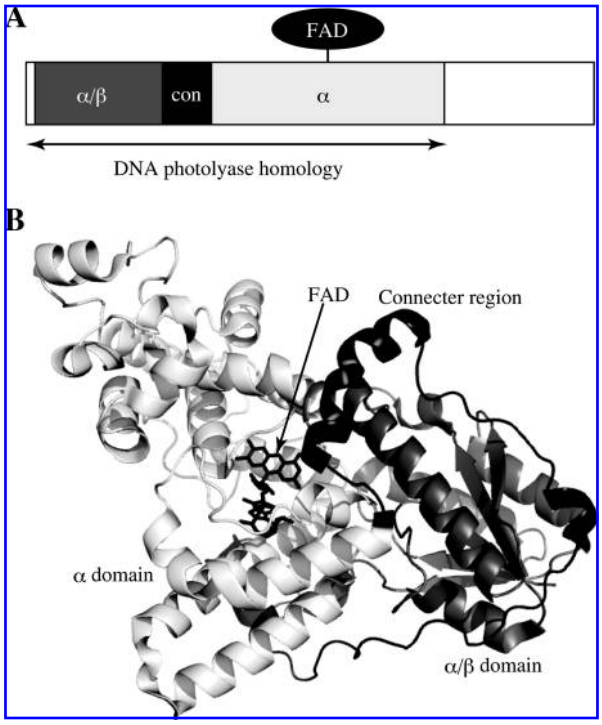

FIG. 11. Cryptochrome. (**A**) A schematic view of the primary structure of cryptochrome. The *black region* labeled as "con" represents the connecter region (domain). (**B**) Crystal structure of the cryptochrome, which has essentially the same fold as that of DNA photolyase. The α/β connecter, and α domains are shown in *dark gray*, *black* and *light gray*, respectively.

D. Flavodoxin

Flavodoxin (149) was first isolated as a flavoprotein with ferredoxin activity from *Clostridium pasteurianum* grown in an iron-deficient medium (86). In most cyanobacteria and algae, flavodoxin functions as an electron-transfer protein under iron-deficient conditions (158). Early in the study of its structure, flavodoxin was successfully crystallized in both oxidized and semiquinone forms (87, 106), and its redox-dependent conformational change has long been known.

Flavodoxin from *C. pasteurianum* is one of the most intensively studied flavodoxins. The crystal structure of flavodoxin was reported in 1972 (3, 105, 183). Flavodoxin is composed of a central 5-stranded β-sheet flanked on either side by α-helices (Fig. 12A). FMN is bound at the top of the molecule and is therefore quite exposed to solvent. The isoalloxazine ring is flanked by two loop regions, and the *re* side of the isoalloxazine ring faces the inside the molecule. The *si* side of the isoalloxazine ring is shielded by a side-chain of a Trp residue (Fig. 12B). In other flavodoxins, this Trp is frequently replaced with Tyr. In the oxidized form of flavodoxin (107), only the O2 and O4 atoms of the isoalloxazine ring form hydrogen bonds with main-chain amide protons. No hydrogen bond was found at the N5 atom. A striking feature of the *C. pasteurianum* flavodoxin in the oxidized state is the *cis*-peptide bond between Gly57 and Asp58, which are located $\sim$5 Å from the N5 atom. This *cis*-peptide converts to a *trans*-peptide in the hydroquinone and semiquinone forms of the flavodoxin, resulting in the formation of a hydrogen bond between the N5 hydrogen and the carbonyl oxygen of Gly57 (Fig. 12B).

Crystallographic analysis revealed similar redox-dependent conformational changes in other flavodoxins from *Desulfovibrio vulgaris* (184) and *Anacystic nidulans* (67). NMR analyses using ^{13}C, ^{15}N, and ^{31}P also supported the rearrangement of the hydrogen bond network around the N5 atom of flavodoxin in solution (175–177). Due to this peptide bond flip, the conformation of the loop region differs between oxidized and reduced forms of flavodoxin.

What is the functional role of the redox-dependent conformational change in the loop region? Since no three-dimensional structures of the complex between flavodoxin and its electron transfer partner are at present available, a comparative analysis of flavodoxin and ferredoxin is useful to predict the functional significance of the redox-dependent peptide flip. Biochemical and NMR spectroscopic studies of

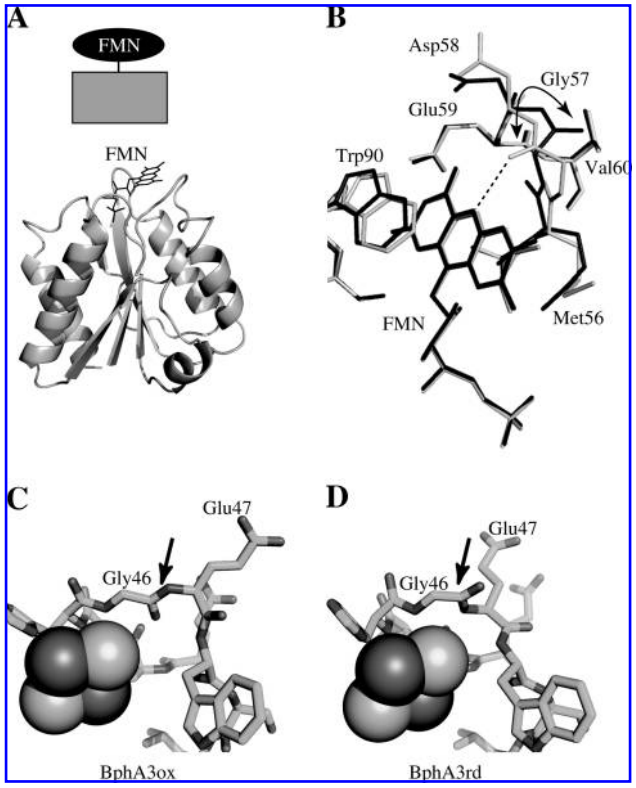

FIG. 12. Flavodoxin and ferredoxin. (**A**) A schematic view of the primary structure of flavodoxin and its crystal structure. (**B**) Redox-dependent main-chain flip observed in the flavodoxin derived from *C. pasteurianum*. Oxidized and reduced forms of flavodoxin are shown in *black* and *light gray*. (**C**, **D**) Redox-dependent main-chain flip observed in the ferredoxin BphA3 derived from *Acidvorax* sp. strain KKS102. (**C**) and (**D**) show the oxidized and reduced form of BphA3, respectively. The [2Fe–2S] clusters in (**C**) and (**D**) are shown in sphere models.

flavodoxin showed that the surface area, including a flipping peptide bond, is involved in the interaction with its electron transfer counterpart (52, 57, 126). Notably, crystal structure analyses of ferredoxins have revealed that a peptide bond close to the [2Fe–2S] cluster also flipped upon reduction of the [2Fe–2S] cluster (123, 154, 159). The surface area containing the flipping peptide bond is also known to be involved in the interaction with redox partners of ferredoxin (Fig. 12C and D) (91, 124, 154). Taking into account the fact that flavodoxin functions as a replacement of ferredoxins under an iron-deficient environment, the redox-controlled flip occurring in the binding site for target proteins might be a common mechanism shared by ferredoxin and flavodoxin to carry out redox-dependent interactions with the partner proteins. Further analysis will be important to fully reveal the functional significance of the redox-dependent peptide bond flip occurring close to the binding site.

E. Ferredoxin reductase

Ferredoxin (Fdx) and ferredoxin reductase (FNR), as well as their relatives, are widely utilized electron-transfer systems in cells. Typically, Fdx and FNR contain an iron–sulfur cluster and an FAD as their redox centers, respectively. The most intensively studied Fdx–FNR systems are those of the photosynthetic system (2, 5, 152). In photosynthesis, two electrons are provided sequentially from the reduced form of Fdx to FNR. The fully reduced FNR, in turn, donates a hydride to $NADP^+$ to produce NADPH. Other well-known Fdx–FNR systems are electron-transfer systems of various oxygenases, including cytochrome P450 (61) and aromatic compound dioxygenase (110). In these cases, electrons derived from NAD(P)H are transferred to the terminal oxygenase by the Fdx–FNR system. The direction of the electron transfer is opposite to that of the photosystem; FNR provides an electron to Fdx. Since these two types of Fdx–FNR systems have distinct properties, both in protein structure and function, they are reviewed separately below.

1. Plant-type ferredoxin reductase in photosynthetic system. Fdx and FNR in photosynthetic systems have long been studied. The studies performed at the initial stage of the research revealed the stoichiometry and redox-dependent nature of the interactions between Fdx and FNR (6–9): (a) one Fdx binds to one FNR, (b) the redox state of Fdx strongly affects its association with FNR, (c) Fdx, FNR, and NADPH/$NADP^+$ form an unstable ternary complex, and (d) the binding of NADPH to FNR seems to facilitate a dissociation of Fdx from FNR. More recent biochemical analysis clearly demonstrated the redox-dependent interaction between Fdx and FNR (23). This interaction is also dependent on $NADP^+$. It is reasonable to expect that the interactions between these proteins are controlled in a redox-dependent manner through protein conformational changes linked to the redox states of the iron–sulfur cluster of Fdx and the FAD of FNR.

In order to reveal the electron-transfer mechanism and the redox-dependent interactions, crystal structure analyses of Fdx and FNR have been intensively performed. The first crystal structure of a plant-type FNR in the oxidized form was determined in 1991 using spinach FNR (Fig. 13A and B) (78). Spinach FNR is composed of two domains, the FAD- and NADPH-binding domains. The FAD molecule in the FNR mainly interacts with the FAD-binding domain. The isoalloxazine ring of the FAD is sandwiched by the two domains. On the basis of the structure of oxidized FNR in complex with 2′-phospho-AMP, it was suggested that the nicotinamide ring of $NADP^+$ is located at the *re* side of the isoalloxazine ring (21, 78). Since the *re* side of the isoalloxazine ring is covered with the side chain of Tyr314, which is the conserved C-terminal residue of the plant-type FNR, the nicotinamide moiety of $NADP^+$ seems to conflict with the side chain of Tyr314 when $NADP^+$ binds to the oxidized form FNR. Indeed, none of the obtained crystal structures of the wild-type FNR and $NADP^+$ complex have shown interaction between the nicotinamide ring of $NADP^+$ and the isoalloxazine ring of FAD. It is obvious that the C-terminal Tyr must move away from the *re* side of the isoalloxazine ring when FNR and $NADP^+$ form a productive electron-transfer complex. The first crystal structure of the FNR–$NADP^+$ complex was determined by the Karplus group by utilizing a mutant for the C-terminal Tyr residue (24). The mechanism of the Tyr shift, however, remains elusive.

Crystal structures of the Fdx–FNR complex were reported by two separate groups (Fig. 13C) (91, 124). In these complexes, both Fdx and FNR were in the oxidized form. Although the Fdx-binding sites on FNR were nearly the same in the two complex structures, the orientations of the Fdx with respect to FNR were marginally different. As shown Fig. 13C,

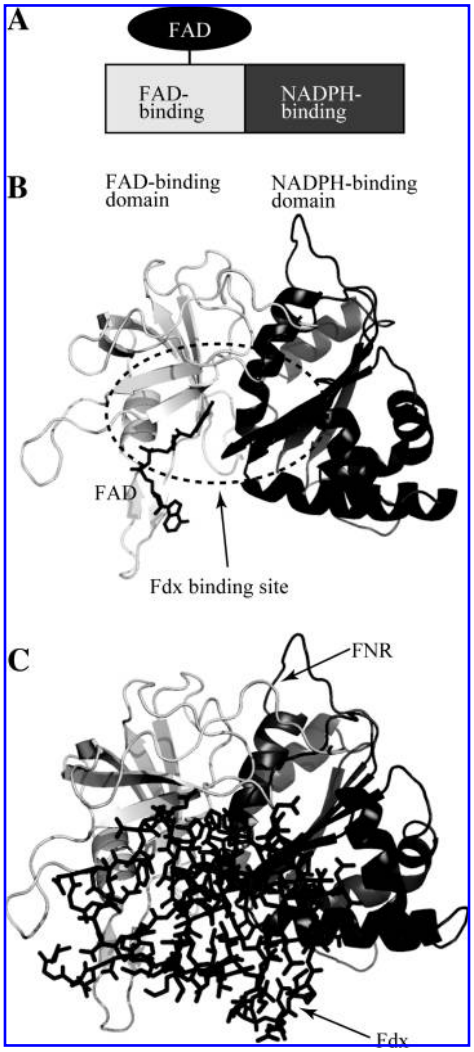

FIG. 13. Plant-type ferredoxin reductase. (**A**) A schematic view of the primary structure of plant-type ferredoxin reductase. (**B**) Crystal structure of ferredoxin reductase from spinach. The FAD-binding and NADPH-binding domains are shown in *light* and *dark gray*, respectively. The *dotted ellipsoid* indicates the ferredoxin-binding site. (**C**) Crystal structure of the ferredoxin–ferredoxin reductase complex from a maize leaf (91). Ferredoxin reductase (FNR) and ferredoxin (Fdx) are shown in *cartoon* and *stick models*, respectively.

Fdx binds FNR from the xylene moiety side of the FAD in both structures. Since the redox centers of Fdx and FNR are located close to the interacting surface of each protein, it is reasonable to predict that redox-dependent changes in the conformational and chemical properties around the FAD of FNR and the [2Fe–2S] cluster of Fdx affect the interaction between Fdx and FNR. In fact, biochemical analyses have revealed that the interaction between FNR and Fdx is mainly controlled by the redox state of Fdx (6). It was also demonstrated that Fdx underwent two types of conformational change in a redox-dependent manner. The first one is a flip of the main-chain peptide bond (123), and the second is a conformational change of the C-terminal region (92). These conformational changes are likely to be involved in the redox-dependent interaction between FNR and Fdx.

The redox-dependent peptide-bond flip was proposed to be important for the dissociation of Fdx from FNR. There are three reports showing that the reduction of Fdx (including bacterial-type Fdx) induces a flip of a peptide bond close to the [2Fe–2S] cluster (123, 154, 159). In Fdx from the cyanobacterium *Anabaena* PCC7119, the peptide bond between Cys46 and Ser47 was found to be flipped upon reduction (123). The flipped peptide bond is located adjacent to Phe65, which is involved in the hydrophobic interaction with FNR (124). Since the flip of the peptide bond seems to induce a conformational change around the Phe residue, Molares *et al*. suggested that, after the electron transfer from FNR to Fdx, this peptide bond flip weakens the affinity between FNR and Fdx to facilitate the dissociation of Fdx from FNR (124). The maize-leaf Fdx–FNR complex (91) may have a similar type of mechanism for the redox-dependent interaction, despite the differences between the two complex structures.

The redox-dependent conformational change of the C-terminal region was proposed on the basis of NMR analysis of Fdx from *Equisetum arvense* (92). In the oxidized Fdx, the C-terminal region seems to adopt a rather extended structure, whereas this region adopts a helical structure in the reduced form of Fdx (92). This conformational change might be responsible for the high-affinity binding between FNR and reduced Fdx.

We cannot exclude the possibility that a redox-dependent conformational change also occurs in plant-type FNR, but so far no clear evidence for it has been obtained. Although a crystal structure analysis of the reduced form of spinach FNR was reported, no significant conformational changes were observed between the oxidized and reduced forms. How-

FIG. 14. Bacterial ferredoxin reductase BphA4 in the biphenyl dioxygenase. (**A**) A schematic view of the primary structure of BphA4. (**B**) Crystal structure of BphA4, which is composed of three domains. The FAD-binding, NADH-binding, and C-terminal domains are shown in *green*, *pink*, and *cyan*, respectively. (**C**) *Top panel* shows that the rigid body rotation of the NADH/CT domain observed in each state (schematic representations). The isoalloxazine rings of FAD are shown in *blue lines*. *Black arrows* in this panel show the direction of the rotation. *Middle* and *bottom panels* show conformational changes of FAD in oxidized (ox), hydroquinone (rd), semiquinone (sq), and re-oxidized (re-ox) states. The simulated-annealing-omit maps for FAD are also shown. The electron density was contoured at the 3.0 σ level. (**D**) Redox-dependent conformational change around the isoalloxazine ring. Oxidized and semiquinone forms are shown in *orange* and *blue*, respectively. (**E**) The mechanism of the NADH/CT domain rotation. The breakage of the hydrogen bond between Lys53 and the N5 atom in FAD induces the domain rotation. (**F**) Redox-dependent domain rotation observed in BphA4. The rotation of the NADH/CT domain regulates the interaction between BphA3 and BphA4. The rotation of the NADH/CT domain avoids its close contact with Ala371 in BphA4 and BphA3. Colors of domains in panels (**C**), (**E**), and (**F**) are the same as those of panel (**B**). Panels (**C**), (**D**), and (**E**) were transferred from reference 154 with some modifications.

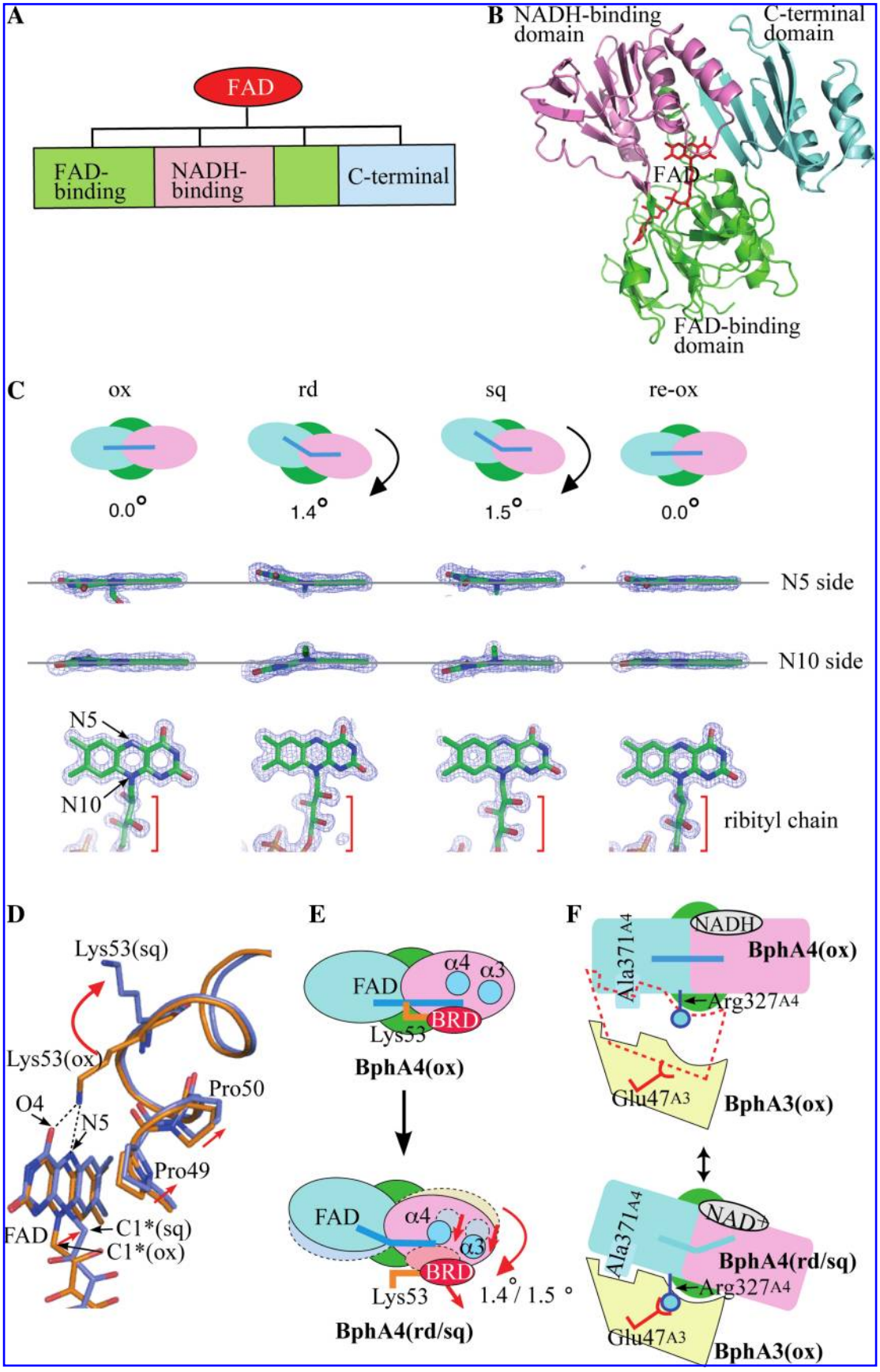
A
FAD
FAD-binding
NADH-binding
C-terminal
B NADH-binding domain
C-terminal domain
FAD
FAD-binding domain
C
ox
rd
sq
re-ox
0.0°
1.4°
1.5°
0.0°
N5 side
N10 side
N5
N10
ribityl chain
D
Lys53(sq)
Lys53(ox)
Pro50
O4
N5
Pro49
FAD
C1*(sq)
C1*(ox)
E
FAD
α4
α3
BRD
Lys53
BphA4(ox)
FAD
α4
α3
BRD
Lys53
1.4 / 1.5 °
BphA4(rd/sq)
F
NADH
BphA4(ox)
Ala371A4
Arg327A4
Glu47A3
BphA3(ox)
NAD+
BphA4(rd/sq)
Ala371A4
Arg327A4
Glu47A3
BphA3(ox)

ever, the FNR in the crystal seemed to be only partially reduced. The crystal structure of hydroquinone-form FNR would be more relevant for examining the details of the redox-dependent interaction between FNR and Fdx.

2. Bacterial ferredoxin reductase in aromatic compound dioxygenase system. In bacteria, there are several dioxygenase systems that are involved in the metabolism of various organic compounds. The BphA enzyme system from *Acidovorax* (*Pseudomonas*) sp. strain KKS102 (83), which catalyzes hydroxylation of biphenyls and polychlorinated biphenyls (43), is composed of three proteins (complexes), BphA1A2, BphA3, and BphA4 (82). Of the three, BphA1A2 is a terminal oxygenase complex that has a catalytic center for the hydroxylation of aromatic compounds. Since this dioxygenase requires two electrons for its catalytic reaction, an electron-transfer system that is composed of BphA3 (Fdx) and BphA4 (FNR) is necessary. The electrons transferred in this system originate from NADH. Initially, BphA4 obtains two electrons from NADH as a form of a hydride ion, resulting in the fully reduced form of FAD in BphA4. The reduced BphA4 transfers one electron each to two BphA3 molecules. The reduced BphA3 molecules then shuttle the electrons to the terminal BphA1A2 oxygenase complex. Similar electron–transfer systems have been found in various organisms. For example, cytochrome P450 systems of *Pseudomonas putida* (88, 142, 160) and adrenal glands (60, 144, 196) contain a similar electron-transfer system consisting of Fdx- and FNR-types of proteins.

We have studied the tertiary structures of BphA3 and BphA4 in order to elucidate the electron–transfer mechanism between them. Crystallographic analysis of BphA4 revealed that BphA4 is composed of three domains, an FAD-binding (residues 1–111, and 238–317), an NADH-binding (residues 112–237), and a C-terminal domain (residues 318–408) (Fig. 14A and B) (157). The FAD molecule is tightly bound to the FAD-binding domain. The isoalloxazine ring of the FAD is located at nearly the center of the molecule and interacts with all three domains. The FAD-binding domain contains a subdomain showing a backrest-shaped structure that is tethered to the isoalloxazine ring through hydrogen bonds in the oxidized-form BphA4. The backrest subdomain (residues 46–65) also interacts with the NADH-binding domain (154).

Recently, biochemical analysis revealed that there is a redox-dependent interaction between BphA3 and BphA4 (154), which seems to be important to promote efficient electron transfer between them. The affinity of BphA4 for BphA3 was increased about 20-fold upon reduction of BphA4. In order to analyze the molecular mechanism of the redox-dependent interaction between BphA3 and BphA4 on the basis of their tertiary structures, we determined the crystal structures of BphA3 (oxidized and reduced forms), BphA4 (oxidized, hydroquinone, blue-semiquinone, and re-oxidized forms), and the BphA3–BphA4 complex (153–155). These crystal structures and biochemical analyses enabled us to present a model of the redox-dependent interaction between them.

Figure 14C summarizes the redox-dependent changes of the overall structure of BphA4 and those of the FAD molecule (154). As shown in the top panel of Fig. 14C, the NADH-binding and C-terminal domains (NADH/CT domain) of BphA4 undergo rigid-body rotation of $\sim 1.5^{\circ}$ with respect to the FAD-binding domain upon BphA4 (FAD) reduction. The rotation mechanism of the NADH/CT domain was explained by the rearrangement of the interaction between FAD and the protein (154). In the oxidized form, Lys53 forms a hydrogen bond with the N5 atom of FAD. Crystal structures of the hydroquinone and semiquinone forms, however, showed that the hydrogen bond was broken probably due to a hydride transfer from NADH to the N5 atom of FAD (Fig. 14D). Since the hydrogen bond between Lys53 and the N5 atom tethers the backrest subdomain to FAD, the loss of the hydrogen bond should increase the mobility of the subdomain. The conformation of the "mobile" backrest subdomain seemed to be changed through the interaction with FAD, which undergoes redox-dependent conformational changes. In the hydroquinone and semiquinone states, the C1* atom of the ribityl chain and the isoalloxazine ring are shifted backward, pushing on Pro49 of the backrest subdomain (Fig. 14D). The backward shift of the backrest subdomain, in turn, seems to cause the shifts of the two α-helices (α2 and α4 helices) in the NADH-binding domain (Fig. 14E) (154). The binding of the nicotinamide ring in front of the isoalloxazine ring seems also to induce the shift of the α4-helix, as observed in the crystal structure of the semiquinone form. The resultant shifts of the helices further induce a rigid body rotation of the NADH/CT domain (Fig. 14E).

The crystal structure of the BphA3–BphA4 complex demonstrated that the BphA3-binding site of BphA4 is composed of the FAD-binding and C-terminal domains (Fig. 14F) (154, 156). Since the rotation of the NADH/CT domain in BphA4 changes the relative orientation of the FAD-binding and C-terminal domains, the reduction of BphA4 induces a conformational change of its BphA3-binding site. In addition, a comparison of the structures of free BphA4 in various redox states and of BphA4 in the BphA3–BphA4 complex showed that rotation is required to avoid close contact between Ala371 of BphA4 and the BphA4-binding surface of BphA3 during the complex formation (Fig. 14F). Thus, the redox-induced rotation of the NADH/CT domain of BphA4 is likely to be required to form a high-affinity binding site for BphA3.

This model is, to the best of our knowledge, the first one explaining a redox-dependent interaction between electron-transfer proteins on the basis of high-resolution crystal structures of their reaction intermediates. The crystal structures, however, seemed to show some effects from the crystal packing and/or the pH (5.3) of the crystal (154). The absorption spectrum of the hydroquinone BphA4–NAD^+ complex in a single crystal and that in solution at pH 5.35 did not show a charge-transfer band, possibly due to protonation of the isoalloxazine ring. Further research employing spectroscopic analysis in solution would lead to a comprehensive understanding of the redox-dependent interaction between BphA3 and BphA4.

VI. Future Research Directions

In this review, we focused on the redox control of flavoprotein conformation, particularly that which is involved in biological signaling including electron transfer. Because of the intensive study of chemical properties of flavin, most of the biochemical phenomena occurring at the flavin moiety of the protein have been well explained, although there are still unsolved problems, such as fast photochemical processes in the photoreceptors. Combined analyses of the tertiary struc-

ture and detailed spectroscopic properties of flavoproteins will reveal much more about functional roles of flavin in these proteins.

Biological signaling by flavoproteins is composed of the following three major steps. The first step is the conversion of the initial chemical event occurring at the flavin site into a structural signal within the flavoprotein. As shown in the present article, the mechanism by which the initial event is "converted" into structural information has been revealed for various flavoproteins by structural and biochemical analyses of reaction intermediates of flavin-containing domains. These molecular switches can be categorized into five distinct types (see Section IV).

The second step is the transduction (or propagation) of the structural signal to the effector site of the protein. In order to analyze the structural signal propagation, a comparison between the structures of the protein in different redox-dependent functional states is essential. However, in some cases such as the PutA protein (98, 192), crystallographic analysis revealed only small conformational changes, the magnitudes of which are comparable to the estimated coordinate error, occurring as a result of flavin reduction (or photoexcitation). When the conformational changes are small, it is difficult to analyze the mechanism of the structural signal transduction in the protein molecule from the crystal structures alone. Furthermore, we should pay attention to the effects of the crystal packing and pH of the crystal structure, both of which may affect the conformations of the protein in the crystals (154). It is therefore important to compare the crystallographic observations with those obtained from experiments carried out in solution, such as spectroscopic and biochemical analyses.

We should pay attention to the possibility that redox-dependent changes in the dynamic properties of the flavin-binding domain play a role in the signal propagation within the protein molecule. Since X-ray crystallography usually cannot provide information about the dynamic properties of protein molecules, spectroscopic analysis, such as NMR, may be required to obtain a deeper insight into the structural signal transduction in flavoproteins. Time-resolved spectroscopy is also a powerful method to analyze details of the reaction of flavoproteins. Fast reaction processes in photoreceptors have been successfully analyzed using picosecond-resolution spectroscopy (34, 45, 46).

The third step is a "readout" process of the structural signal transferred to the effector site. There are two types of the signal readout process. One is signal readout by a distinct molecule through the formation of an intermolecular signaling complex, and another is that by domain(s) adjacent to the flavin-containing domain through the adoption of a signaling conformation (in case of the multi-domain flavoproteins). Only a few examples of the tertiary structural analysis of signaling complex/conformation have been reported, probably because in general, the signaling complex/conformation is transiently formed and relatively unstable.

In order to analyze the tertiary structure of a signaling complex, it should be stably isolated under appropriate conditions. To find such conditions to crystallize the signaling complex, it is critical to analyze the biophysical properties of the signaling complex, including the dissociation constant. In case of the BphA3–BphA4 complex, the crystal of the complex could be obtained through mixing reduced BphA4 and oxidized BphA3 under anaerobic conditions, because the reduction of BphA4 increases the affinity for BphA3 (154, 156). In addition, analysis of the dynamic characteristics of a signaling complex by the physicochemical method is important, as exemplified by the molecular weight analysis of the LOV domain in Vivid using gel filtration (197). Static light scattering and analytical ultracentrifugation would also provide useful information about the dynamics of the signaling complexes.

In order to fully understand the structural basis of redox-dependent conformational change in the biological signaling by flavoproteins, structural analysis of reaction intermediates of the whole molecule, as well as the flavin-containing domain, are required. However, most of the structural analyses have been performed using only the FAD-containing domain (29, 30, 98, 192) and have failed to detect the conformational changes expected by biochemical observation. Crystal structure analysis of the whole molecule is an important challenge in this field. Combined analyses with electron microscopy and/or small-angle X-ray scattering could contribute significantly to this effort.

In order to further analyze the redox-dependent conformational changes of flavoproteins, we shall discuss the energy landscape of the flavoprotein conformations. The conformational and/or protonation-state change of the flavin provides small structural perturbations to the inside of the flavoprotein, leading to a conformational change of the whole

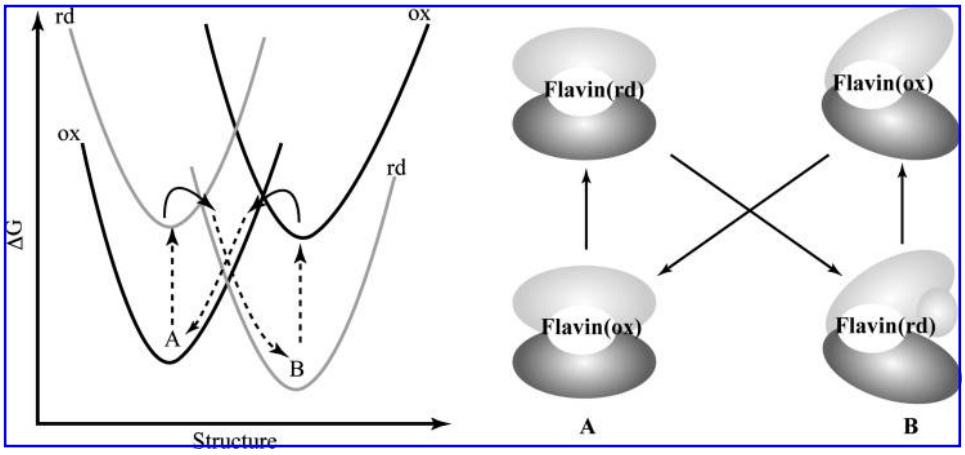

FIG. 15. A schematic energy landscape of the redox-dependent conformational change of the flavoproteins. Labels ox (*black*) and rd (*gray*) in the *left graph* represent the oxidized and reduced forms of the bound flavin, respectively. Conformations of the protein are shown in labels **A** and **B**. The *right panel* shows schematic representations of each state of the molecule appearing in the graph.

flavoprotein molecule in a redox-dependent manner. This process can be explained energetically as shown in Fig. 15. When the binding affinity of a reduced flavin for the apoprotein in the oxidized conformation is weaker than that for the apoprotein in the reduced conformation, the reduction of flavin bound to the apoprotein in the oxidized conformation energetically destabilizes the oxidized conformation relative to the reduced conformation, causing the latter to relax somewhat. The conversion from the reduced to the oxidized conformation can be explained in the same manner supposing that the apoprotein in the oxidized conformation exhibits higher affinity to oxidized flavin than to reduced flavin. Taking into account the fact that some flavin-containing domains show no significant redox-dependent conformational changes, this mechanism should be considered in terms of the whole molecule. In addition, in order to demonstrate this type of conformational change, the protein must have at least two meta-stable structural states that are in a reversible equilibrium as shown schematically in Fig. 15. Identifying the structural features that enable the existence of two (or more) meta-stable conformations with comparable stability is a future challenge in this field.

VII. Concluding Remarks

In the present review, we summarize the redox-dependent conformational changes of flavoprotein involved in biological signaling. Structural information about the reaction intermediates of the flavoproteins enabled us to categorize the changes proximal to the flavin into five categories. We identify the next challenge in this field as the analysis of the signaling inside and between proteins (or domains) on the basis of the tertiary structures of the flavoproteins (or complexes). How is a small change occurring at the flavin site propagated within the protein to change the conformation of the effector site? How is the conformational change of the effector site recognized by the signaling partner molecule or domain(s)? These are critical questions not only in the study of the redox control of flavoproteins involved in biological signaling, but also in the study of the signaling by protein molecules in general. Since the redox state of flavoproteins can be controlled by a certain reagent (or light) with relative ease, flavoproteins are good candidates for studying intra- and intermolecular signaling. When these physicochemical properties are well understood, deeper insights into protein signaling will be obtained.

Acknowledgments

This study was partly supported by Grants-in-Aid from the New Energy and Industrial Technology Development Organization (NEDO) of Japan, and the Ministry of Education, Culture, Sports, Science, and Technology of Japan.

Abbreviations

AIF, apoptosis-inducing factor; ADP, adenosine diphosphate; AMP, adenosine 5′-phosphate; AppA, activation of photopigment and *puc* expression; BLUF, blue-light-using flavin adenine dinucleotide; BRD, backrest subdomain; CCP4, collaborative computational project, number 4; CRY, cryptochrome; DBD, DNA-binding domain; DNA, deoxyribonucleic acid; FAD, flavin adenine dinucleotide; Fdx, ferredoxin; FMN, flavin mononucleotide; FNR, ferredoxin reductase; GR, glutathione reductase; LOV, light-oxygen-voltage; MICAL, molecule interacting with CasL; NADH, nicotinamide adenine dinucleotide; NADH/CT domain, NADH-binding and C-terminal domains; NADPH, nicotinamide adenine dinucleotide phosphate; NMDAR, *N*-methyl-D-aspartate type glutamine receptors; NMR, nuclear magnetic resonance; P5CDH, NAD^+-dependent Δ^1-pyrroline-5-carboxylate dehydrogenase; PAS, Per-ARNT-Sim; PAC, photoactivated adenylyl cyclase; PDB, protein data bank; PHY, phytochrome; PRODH, FAD-containing proline dehydrogenase; PSI, photosystem I; putA, proline utilization A; putP, proline utilization P; rmsd, root-mean square deviation; UDP, uridine 5′-diphosphate.

References

1. Ahmad M and Cashmore AR. HY4 gene of *A. thaliana* encodes a protein with characteristics of a blue-light photoreceptor. *Nature* 366: 162–166, 1993.
2. Aliverti A, Pandini V, Pennati A, de Rosa M, and Zanetti G. Structural and functional diversity of ferredoxin-$NADP^+$ reductase. *Arch Biochem Biophys* 474: 283–291, 2008.
3. Andersen RD, Apgar PA, Burnett RM, Darling GD, Lequesne ME, Mayhew SG, and Ludwig ML. Structure of the radical form of clostridial flavodoxin: A new molecular model. *Proc Natl Acad Sci USA* 69: 3189–3191, 1972.
4. Anderson S, Dragnea V, Masuda S, Ybe J, Moffat K, and Bauer C. Structure of a novel photoreceptor, the BLUF domain of AppA from *Rhodobacter sphaeroides*. *Biochemistry* 44: 7998–8005, 2005.
5. Arakaki AK, Ceccarelli EA, and Carrillo N. Plant-type ferredoxin-$NADP^+$ reductases: a basal structural framework and a multiplicity of functions. *FASEB J* 11: 133–140, 1997.
6. Batie CJ and Kamin H. The relation of pH and oxidation-reduction potential to the association state of the ferredoxin-ferredoxin:$NADP^+$ reductase complex. *J Biol Chem* 256: 7756–7763, 1981.
7. Batie CJ and Kamin H. Ferredoxin:$NADP^+$ oxidoreductase: Equilibria in binary and ternary complexes with $NADP^+$ and ferredoxin. *J Biol Chem* 259: 8832–8839, 1984.
8. Batie CJ and Kamin H. Electron transfer by ferredoxin:$NADP^+$ reductase: rapid-reaction evidence for participation of a ternary complex. *J Biol Chem* 259: 11976–11985, 1984.
9. Batie CJ and Kamin H. Association of ferredoxin-NADP+ reductase with NADP(H) specificity and oxidation-reduction properties. *J Biol Chem* 261: 11214–11223, 1986.
10. Beinert W-D, Rüterjans H, and Müller F. Nuclear magnetic resonance studies of the old yellow enzyme 1. ^{15}N NMR of the enzyme recombined with ^{15}N-labeled flavin mononucleotides. *Eur J Biochem* 152: 573–579, 1985.
11. Beinert W-D, Rüterjans H, Müller F, and Bacher A. Nuclear magnetic resonance studies of the old yellow enzyme 2. ^{13}C NMR of the enzyme recombined with ^{13}C-labeled flavin mononucleotides. *Eur J Biochem* 152: 581–587, 1985.
12. Beis K, Srikannathasan V, Liu H, Fullerton SWB, Bamford VA, Sanders DAR, Whitfield C, McNeil MR, and Naismith JH. Crystal structure of *Mycobacteria tuberculosis* and *Klebsiella pneumoniae* UDP-galactopyranose mutase in the oxidized state and *Klebsiella pneumoniae* UDP-galactopyranose mutase in the (active) reduced state. *J Mol Biol* 348: 971–982, 2005.

13. Berman HM, Westbrook J, Feng Z, Gilliland G, Bhat TN, Weissig H, Shindyalov IN, and Bourne PE. The protein data bank. *Nucleic Acid Res* 28: 235–242, 2000.
14. Binda C, Coda A, Angelini R. Federico R, Ascenzi P, and Mattevi A. A 30Å long U-shaped catalytic tunnel in the crystal structure of polyamine oxidase. *Structure* 7: 265–276, 1999.
15. Binda C, Newton–Vinson P, Hubalek F, Edmondson DE, and Mattevi A. Structure of human monoamine oxidase B, a drug target for the treatment of neurological disorders. *Nat Struct Biol* 9: 22–26, 2002.
16. Bourgeois D and Royant A. Advances in kinetic protein crystallography. *Curr Opin Struct Biol* 15: 538–547, 2005.
17. Brautigam, CA, Smith BS, Ma Z, Palnitkar M, Tomchick DR, Machius M, and Deisenhofer J. Structure of the photolyase-like domain of cryptochrome 1 from *Arabidopsis thaliana*. *Proc Natl Acad Sci USA* 101: 12142–12147, 2004.
18. Briggs WR, Christie JM, and Salomon M. Phototropins: Aa new family of flavin-binding blue light receptors in plants. *Antioxid Redox Signal* 3: 775–788, 2001.
19. Brown ED and Wood JM. Conformational change and membrane association of the PutA protein are coincident with reduction of its FAD cofactor by proline. *J Biol Chem* 268: 8972–8979, 1993.
20. Brudler R, Hitomi K, Daiyasu H, Toh H, Kucho K, Ishiura M, Kanehisa M, Roberts VA, Todo T, Tainer JA, and Getzoff ED. Identification of a new cryptochrome class: Structure, function, and evolution. *Mol Cell* 11: 59–67, 2003.
21. Bruns CM and Karplus PA. Refined crystal structure of spinach ferredoxin reductase at 1.7 Å resolution: oxidized, reduced and 2′-phospho-5′-AMP bound states. *J Mol Biol* 247: 125–145, 1995.
22. Busza A, Emery–Le M, Rosbash M, and Emery P. Roles of the two *Drosophila* CRYPTOCHROME structural domains in circadian photoreception. *Science* 304: 1503–1506, 2004.
23. Cassan N, Lagoutte B, and Sétif P. Ferredoxin-$NADP^+$ reductase. Kinetics of electron transfer, transient intermediates, and catalytic activities studied by flash-absorption spectroscopy with isolated photosystem I and ferredoxin. *J Biol Chem* 280: 25960–25972, 2005.
24. Ceccarelli EA, Carrillo N, and Karplus PA. A productive $NADP^+$ binding mode of ferredoxin-$NADP^+$ reductase revealed by protein engineering and crystallographic studies. *Nat Struct Biol* 6: 847–853, 1999.
25. Christie JM, Reymond P, Powell GK, Bernasconi P, Raibekas AA, Liscum E, and Briggs WR. *Arabidopsis* NPH1: A flavoprotein with the properties of a photoreceptor for phototropinsm. *Science* 282: 1698–1701, 1998.
26. Christie JM, Salomon M, Nozue K, Wada M, and Briggs WR. LOV (light, oxygen, or voltage) domains of the blue-light photoreceptor phototropin (nph1): binding sites for the chromophore flavin mononucleotide. *Proc Natl Acad Sci USA* 96: 8779–8783, 1999.
27. Churbanova IY and Sevrioukova IF. Redox-dependent changes in molecular properties of mitochondrial apoptosis-inducing factor. *J Biol Chem* 283: 5622–5631, 2008.
28. Collaborative computational project, number 4. The CCP4 suite: Programs for protein crystallography. *Acta Crystallogr* D50: 760–763, 1994.
29. Crosson S and Moffat K. Structure of a flavin-binding plant photoreceptor domain: Insights into light-mediated signal transduction. *Proc Natl Acad Sci USA* 98: 2995–3000, 2001.
30. Crosson S and Moffat K. Photoexcited structure of a plant photoreceptor domain reveals a light-driven molecular switch. *Plant Cell* 14: 1067–1075, 2002.
31. Dissel S, Codd V, Fedic R, Garner KJ, Costa R, Kyriacou CP, and Rosato E. A constitutively active cryptochrome in *Drosophila melanogaster*. *Nat Neuroscience* 7: 834–840, 2004.
32. Dixon DA, Lindner DL, Branchaud B, and Lipscomb WN. Conformations and electronic structures of oxidized and reduced isoalloxazine. *Biochemistry* 18: 5770–5775, 1979.
33. Domratcheva T, Grigorenko BL, Schlichting I, and Nemukhin AV. Molecular models predict light-induced glutamine tautomerization in BLUF photoreceptors. *Biophysical J* 94: 3872–3879, 2008.
34. Dragnea V, Waegele M, Balascuta S, Bauer C, and Dragnea B. Time-resolved spectroscopic studies of the AppA blue-light receptor BLUF domain from *Rhodobacter shaeroides*. *Biochemistry* 44: 15978–15985, 2005.
35. Dym O and Eisenberg D. Sequence-structure analysis of FAD-containing proteins. *Protein Sci* 10: 1712–1728, 2001.
36. Eisenreich W, Kemter K, Bacher A, Mulrooney SB, Williams CH Jr, and Müller F. ^{13}C-, ^{15}N- and ^{31}P-NMR studies of oxidized and reduced low molecular mass thioredoxin reductase and some mutant proteins. *Eur J Biochem* 271: 1437–1452, 2004.
37. Entsch B, Ballou DP, and Massey V. Flavin-oxygen derivatives involved in hydroxylation by p-hydroxybenzoate hydroxylase. *J Biol Chem* 251: 2550–2563, 1976.
38. Entsch B, Cole LJ, and Ballou DP, Protein dynamics in the function of *p*-hydroxybenzoate hydroxylase. *Arch Biochem Biophys* 433: 297–311, 2005.
39. Farmer EE. Surface-to-air signals. *Nature* 411: 854–856, 2001.
40. Fleischmann G, Lederer F, Müller F, Bacher A, and Rüterjans H. Flavin–protein interactions in flavocytochrome b_2 as studied by NMR after reconstitution of the enzyme with ^{13}C- and ^{15}N-labelled flavin. *Eur J Biochem* 267: 5156–5167, 2000.
41. Fraaije MW and Mattevi A. Flavoenzumes: Diverse catalysts with recurrent features. *Trends Biochem Sci* 28:283–296, 2000.
42. Fritchie CJ Jr and Johnston RM. Molecular complexes of flavins. The crystal structure of lumiflavin-bis(naphthalene-2,3-diol) trihydrate. *Acta Cryst* B31: 454–461, 1975.
43. Fukuda M, Yasukouchi Y, Kikuchi Y, Nagata Y. Kimbara K, Horiuchi H, Takagi M, and Yano K. Identification of the *bphA* and *bphB* genes of *Pseudomonas* sp. strain KKS102 involved in degradation of biphenyl and polychlorinated biphenyls. *Biochem Biophys Res Commun* 202: 850–856, 1994.
44. Gatti DL, Palfey BA, Lah MS, Entsch B, Massey V, Ballou DP, and Ludwig ML. The mobile falvin of 4-OH benzoate hydroxylase. *Science* 266: 110–114, 1994.
45. Gauden M, Grinstead JS, Laan W, van Stokkum IHM, Avila–Perez M, Toh KC, Boelens R, Kaptein R, van Grondelle R, Hellingwerf KJ, and Kennis JTM. On the role of aromatic side chains in the photoactivation of BLUF domains. *Biochemistry* 46: 7405–7415, 2007.
46. Gauden M, van Stokkum IHM, Key JM, Lührs DC, van Grondelle R, Hegemann P, and Kennis JTM. Hydrogen-bond switching through a radical pair mechanism in a flavin-binding photoreceptor. *Proc Natl Acad Sci USA* 103: 10895–10900, 2006.
47. Gauden M, Yeremenko S, Laan W, van Stokkum IH, Ihalainen JA, van Grondelle R, Hellingwerf KJ, and Kennis JT.

Photocycle of the flavin-binding photoreceptor AppA, a bacterial transcriptional antirepressor of photosynthesis genes. *Biochemistry* 44: 3653–3662, 2005.
48. Ghisla S, Massey V, Lhoste J–M, and Mayhew SG. Fluorescence and optical characteristics of reduced flavins and flavoproteins. *Biochemistry* 13: 589–597, 1974.
49. Ghisla S and Massey V. Mechanisms of flavoprotein-catalyzed reactions. *Eur J Biochem* 181: 1–17, 1989.
50. Gomelsky M and Klug G. BLUF: A novel FAD-binding domain involved in sensory transduction in microorganisms. *Trends Biochem Sci* 27: 497–500, 2002.
51. Gong W, Hao B, Mansy SS, Gonzalez G, Ailles–Gonzalez MA, and Chan MK. Structure of a biological oxygen sensor: A new mechanism for heme-driven signal transduction. *Proc Natl Acad Sci USA* 95: 15177–15182, 1998.
52. Goñi G, Serrano A, Frago S, Hervás M, Peregrina JR, De la Rosa MA, Gómez–Moreno C, Navarro JA, and Medina M. Flavodoxin-mediated electron transfer from photosystem I to ferredoxin-$NADP^+$ reductase in *Anabaena*: Role of flavodoxin hydrophobic residues in protein–protein interactions. *Biochemistry* 47: 1207–1217, 2008.
53. Griffin KJ, Degala GD, Eisenreich W, Müller F, Bacher A, and Frerman FE. ^{31}P-NMR spectroscopy of human and *Paracoccus denitrificans* electron transfer flavoprotein, and ^{13}C- and ^{15}N-NMR spectroscopy of human electron transfer flavoprotein in the oxidized and reduced states. *Eur J Biochem* 255: 125–132, 1998.
54. Grinstead JS, Aliva–Perez M, Hellingwerf KJ, Boelens R, and Kaptein R. Light-induced flipping of a conserved glutamine side chain and its orientation in the AppA BLUF domain. *J Am Chem Soc* 128: 15066–15067, 2006.
55. Gustafsson TN, Sandalova T, Lu J, Holmgren A, and Schneider G. High-resolution structures of oxidized and reduced thioredoxin reductase from *Helicobacter pylori*. *Acta Crystallogr* D63: 833–543, 2007.
56. Haarer BK and Amberg DC. Old yellow enzyme protects the actin cytoskeletone from oxidative stress. *Mol Biol Cell* 15: 4522–4531, 2004.
57. Hall DA, Kooi CWV, Stasik CN, Stevens SY, Zuiderweg ERP, and Matthews RG. Mapping the interactions between flavodoxin and its physiological partners flavodoxin reductase and cobalamin-dependent methionine synthase. *Proc Natl Acad Sci USA* 98: 9521–9526, 2001.
58. Hall LH, Bowers ML, and Durfor CN. Further consideration of flavin coenzyme biochemistry afforded by geometry-optimized molecular orbital calculations. *Biochemistry* 26: 7401–7409, 1987.
59. Hall LH, Orchard BJ, and Tripathy SK. The structure and properties of flavins: Molecular orbital study based on totally optimized geometries. I. Molecular geometry investigations. *Int J Quantum Chem* 31:195–216, 1987.
60. Hamamoto I, Kurokohchi K, Tanaka S, and Ichikawa Y. Adrenoferredoxin-binding peptide of NADPH-adrenoferredoxin reductase. *Biochim Biophys Acta* 953: 207–213, 1988.
61. Hannemann F, Bichet A, Ewen KM, and Bernhardt R. Cytochrome P450 systems. Biological variations of electron transport chains. *Biochim Biophys Acta* 1770: 330–344, 2007.
62. Harper SM, Neil LC, and Gardner KH. Structural basis of a phototropin light switch. *Science* 301: 1541–1544, 2003.
63. Hasegawa K, Masuda S, and Ono T. Structural intermediate in the photocycle of a BLUF (sensor of Blue Light Using FAD) protein Slr1694 in a Cyanobacterium *Synechocystis* sp. PCC6803. *Biochemistry* 43: 14979–14986, 2004.
64. Heelis PF. The photophysical and photochemical properties of flavins. *Chem Soc Rev* 11: 15–39, 1982.
65. Heintzen C, Loros JJ, and Dunlap JC. The PAS protein VIVID defines a clock-associated feedback loop that represses light input, modulates gating, and regulates clock resetting. *Cell* 104: 453–464, 2001.
66. Hill S, Austin S, Eydmann T, Jones T, and Dixon R. *Azobacter vinelandii* NIFL is a flavoprotein that modulates transcriptional activation of nitrogen-fixation genes via a redox-sensitive switch. *Proc Natl Acad Sci USA* 93: 2143–2148, 1996.
67. Hoover DM, Drennan CL, Metzger AL, Osborne C, Weber CH, Pattridge KA, and Ludwig ML. Comparisons of wild-type and mutant flavodoxins from *Anacystis nidulans*. Structural determinants of the redox potentials. *J Mol Biol* 294: 725–743, 1999.
68. Huala E, Oeller PW, Liscum E, Han IS, Larsen E, and Briggs WR. *Arabidopsis* NPH1: A protein kinase with a putative redox-sensing domain. *Science* 278: 2120–2123, 1997.
69. Huang ZJ, Curtin KD, and Rosbash M. PER protein interactions and temperature compensation of a circadian clock in *Drosophila*. *Science* 267: 1169–1172, 1995.
70. Huang ZJ, Edery I, and Rosbash M. PAS is a dimerization domain common to *Drosophila* period and several transcription factors. *Nature* 364: 259–262, 1993.
71. Ida K, Kurabayashi M, Suguro M, Hiruma Y, Hikima, T, Yamamoto M, and Suzuki H. Structural basis of proteolytic activation of L-phenylalanine oxidase from *Pseudomonas* sp. P-501. *J Biol Chem* 283: 16584–16590, 2008.
72. Iseki M, Matsunaga S, Murakami A. Ohno K, Shiga K, Yoshida K, Sugai M, Takahashi T, Hori T, and Watanabe M. A blue-light-activated adenylyl cyclase mediates photoavoidance in *Euglena gracilis*. *Nature* 415:1047–1051, 2002.
73. Jarillo JA, Gabrys H, Capel J, Alonso JM, Ecker JR, and Cashmore AR. Phototropin related NPL1 controls chloroplast relocation induced by blue light. *Nature* 410: 952–954, 2001.
74. Jung A, Domratcheva T, Tarutina M, Wu Q, Ko W–H, Shoeman RL, Gomelsky M, Gardner K, and Schlichting I. Structure of a bacterial BLUF photoreceptor: Insights into blue light-mediated signal transduction. *Proc Natl Acad Sci USA* 102: 12350–12355, 2005.
75. Jung A, Reinstein J, Domratcheva T, Shoeman RL, and Schlichting I. Crystal structures of the AppA BLUF domain photoreceptor provide insights into blue light-mediated signal transduction. *J Mol Biol* 362: 717–732, 2006.
76. Kagawa T, Sakai T, Suetsugu N, Oikawa K, Ishiguro K, Kato S, Tabata S, Okada K, and Wada M. *Arabidopsis* NPL1: A phototropin homolog controlling the chloroplast high-light avoidance response. *Science* 291: 2138–2141, 2001.
77. Kao Y-T, Saxwna C, He T-F, Guo L, Wang L, Sancar A, and Zhong D. Ultrafast dynamics of flavin in five redox states. *J Am Chem Soc* 130: 13132–13139, 2008.
78. Karplus PA, Daniels MJ, and Herriott JR. Atomic structure of ferredoxin-$NADP^+$ reductase: Prototype for a structurally novel flavoenzyme family. *Science* 251: 60–66, 1991.
79. Karplus PA, Fox KM, and Massey V. Structure–function relationship for old yellow enzyme. *FASEB J* 9: 1518–1526, 1995.
80. Karplus PA and Schulz GE. Refined crystal structure of glutathione reductase at 1.54 Å resolution. *J Mol Biol* 195: 701–729, 1987.
81. Key J, Hefti M, Purcell EB, and Moffat K. Structure of the redox sensor domain of *Azotobacter vinelandii* NifL at atomic resolution: Signaling, dimerization, and mechanism. *Biochemistry* 46: 3614–3623, 2007.

82. Kikuchi Y, Nagata Y, Hinata M, Kimbara K, Fukuda M, Yano K, and Takagi M. Identification of the *bphA4* gene encoding ferredoxin reductase involved in biphenyl and polychlorinated biphenyl degradation in *Pseudomonas* sp. strain KKS102. *J Bacteriol* 176: 1689–1694, 1994.
83. Kimbara K, Hashimoto T, Fukuda M, Koana T, Takagi M, Oishi M, and Yano K. Isolation and characterization of a mixed culture that degrades polychlorinated biphenyls. *Agric Biol Chem* 52: 2885–2891, 1988.
84. Kinoshita T, Doi M, Suetsugu N, Kagawa T, Wada M, and Shimazaki K. Phot1 and phot2 mediate blue light regulation of stomatal opening. *Nature* 414: 656–660, 2001.
85. Kita A, Okajima K, Morimoto Y, Ikeuchi M, and Miki K. Structure of a Cyanobacterial BLUF protein, Tll0078, containing a novel FAD-binding blue light sensor domain. *J Mol Biol* 349: 1–9, 2005.
86. Knight E Jr, D'Eustachio AJ, and Hardy RW. Flavodoxin: a flavoprotein with ferredoxin activity from *Clostridium pasteurianum*. *Biochim Biophys Acta* 113: 626–628, 1966.
87. Knight E Jr and Hardy RWF. Isolation and characteristics of flavodoxin from nitrogen-fixing *Clostridium pasteurianum*. *J Biol Chem* 241: 2752–2756, 1966.
88. Koga H, Yamaguchi E, Matsunaga K, Aramaki H, and Horiuchi T. Cloning and nucleotide sequences of NADH-putidaredoxin reductase gene (*camA*) and putidaredoxin gene (*camB*) involved in cytochrome P-450cam hydroxylase of *Pseudomonas putida*. *J Biochem* 106: 831–836, 1989.
89. Kume K, Zylka MJ, Sriram S, Shearman LP, Weaver DR, Jin X, Maywood ES, Hastings MH, and Reppert SM. mCRY1 and mCRY2 are essential components of the negative limb of the circadian clock feedback loop. *Cell* 98: 193–205, 1999.
90. Kuo MC, Dunn JBR, and Fritchie CJ Jr. The crystal structure of a flavin molecular complex: 10-propylisoalloxazine-bis(naphthalene-2,3-diol). *Acta Cryst* B30: 1766–1771, 1974.
91. Kurisu G, Kusunoki M, Katoh E, Yamazaki T, Teshima K, Onda Y, Kimata–Ariga Y, and Hase T. Structure of the electron transfer complex between ferredoxin and ferredoxin-$NADP^+$ reductase. *Nat Struct Biol* 8: 117–121, 2001.
92. Kurisu G, Nishiyama D, Kusunoki M, Fujikawa S, Katoh M, Hanke GT, Hase T, and Teshima K. A structural basis of *Equisetum arvense* ferredoxin isoform II producing an alternative electron transfer with ferredoxin-$NADP^+$ reductase. *J Biol Chem* 280: 2275–2281, 2005.
93. Kuriyan J, Krishna TS, Wong L, Guenther B, Pahler A, Williams CH Jr, and Model P. Convergent evolution of similar function in two structurally divergent enzymes. *Nature* 352: 172–174, 1991.
94. Kyte J. *Mechanism in Protein Chemistry. New York,* Garland Publishing, New York, 1995, pp. 72–90.
95. Land EJ and Swallow AJ. One-electron reactions in biochemical systems as studied by pulse radiolysis. II. Riboflavin. *Biochemistry* 8: 2117–2125, 1969.
96. Ledwidge R, Patel B, Dong A, Fiedler D, Falkowski M, Zelikova J, Summers AO, Pai EF, and Miller SM. NmerA, the metal binding domain of mercuric ion reductase, removes Hg^{2+} from proteins, delivers it to the catalytic core, and protects cells under glutathione-depleted conditions. *Biochemistry* 44: 11402–11416, 2005.
97. Lee B and Richards FM. The interpretation of protein structures: Estimation of static accessibility. *J Mol Biol* 55: 379–400, 1971.
98. Lee YH, Nadaraia S, Gu D, Becker DF, and Tanner JJ. Structure of the proline dehydrogenase domain of the multifunctional PutA flavoprotein. *Nat Struct Biol* 10: 109–114, 2003.
99. Lennon BW, Williams CH, and Ludwig ML. Crystal structure of reduced thioredoxin reductase from *Escherichia coli*: Structural flexibility in the isoalloxazine ring of the flavin adenine dinucleotide cofactor. *Protein Sci* 8: 2366–2379, 1999.
100. Li J, Vrielink A, Brick P, and Blow DM. Crystal structure of cholesterol oxidase complexed with a steroid substrate: Implications for flavin adenine dinucleotide dependent alcohol oxidase. *Biochemistry* 32: 11507–11515, 1993.
101. Lin C, Robertson DE, Ahmad M, Raibekas AA, Jorns MS, Dutton PL, and Cashmore AR. Association of flavin adenine dinucleotide with the *Arabidopsis* blue light receptor CRY1. *Science* 269: 968–970, 1995.
102. Lin C and Todo T. The cryptochromes. *Genome Biol* 6: 220, 2005.
103. Ling M, Allen SW, and Wood JM. Sequence analysis identifies the proline dehydrogenase and delta 1-pyrroline-5-carboxylate dehydrogenase domains of the multifunctional *Escherichia coli* PutA protein. *J Mol Biol* 243: 950–956, 1994.
104. Lostao A, Harrous ME, Daoudi F, Romero A, Parody–Morreale A, and Sancho J. Dissecting the energetics of the apoflavodoxin-FMN complex. *J Biol Chem* 275: 9518–9526, 2000.
105. Ludwig ML, Andersen RD, Apgar PA, Burnett RM, LeQuesne ME, and Mayhew SG. The structure of a clostridial flavodoxin, an electron–transferring flavoprotein. 3. An interpretation of an electron-density map at a nominal resolution of 3.25 angstrom. *Cold Spring Harb Symp Quant Biol* 36: 369–380, 1972.
106. Ludwig ML, Andersen RD, Mayhew SG, and Massey V. The structure of a Clostridial flavodoxin. *J Biol Chem* 244: 6047-6048, 1969.
107. Ludwig ML, Pattridge KA, Metzger AL, Dixon MM, Eren M, Feng Y, and Swenson RP. Control of oxidation-reduction potentials in flavodoxin from *Clostridium beijerinckii*: The role of conformation changes. *Biochemistry* 36: 1259–1280, 1997.
108. Ma J, Joshimura M, Yamashita E, Nakagawa A, Ito A, and Tsukihara T. Structure of rat monoamine oxidase A and its specific recognitions for substrate and inhibitors. *J Mol Biol* 338: 103–114, 2004.
109. Martineau M, Baux G, and Mothet J–P. D-Serine signaling in the brain: Friend and foe. *Trends Neurosci* 29: 481–491, 2006.
110. Mason JR and Cammack R. The electron-transport proteins of hydroxylating bacterial dioxygenases. *Annu Rev Microbiol* 46: 277–305, 1992.
111. Massey V. The chemical and biological versatility of riboflavin. *Biochem Soc Trans* 28:283–296, 2000.
112. Massey V and Ghisla S. Role of charge-transfer interactions in flavoprotein catalysis. *Ann NY Acad Sci* 227: 446–465, 1974.
113. Massey V and Palmer G. On the existence of spectrally distinct classes of flavoprotein semiquinones. A new method for the quantitative production of flavoprotein semiquinones. *Biochemistry* 5: 3181–3189, 1966.
114. Masuda S and Bauer CE. AppA is a blue light photoreceptor that antirepresses photosynthesis gene expression in *Rhodobacter sphaeroides*. *Cell* 110: 613–623, 2002.
115. Masuda S, Hasegawa K, Ishii A, and Ono T. Light-induced structural change in a putative blue-light receptor with a

novel FAD binding fold sensor of blue-light using FAD (BLUF): Slr1694 of *Synechocystis* sp. PCC6803. *Biochemistry* 43: 5304–5313, 2004.
116. Maté MJ, Ortiz–Lombardía M, Boitel B, Haouz A, Tello D, Susin SA, Penninger J, Kroemer G, and Alzari PM. The crystal structure of the mouse apoptosis-inducing factor AIF. *Nat Struct Biol* 9: 442–446, 2002.
117. Menzel R and Roth J. Purification of the *putA* gene product. *J Biol Chem* 256: 9755–9761, 1981.
118. Menzel R and Roth J. Enzymatic properties of the purified *putA* protein from *Salmonella typhimurium*. *J Biol Chem* 256: 9762–9766, 1981.
119. Modjtahedi N, Giordanetto F, Madeo F, and Kroemer G. Apoptosis-inducing factor: Vital and lethal. *Trends Cell Biol* 16: 264–272, 2006.
120. Moonen CTW, van den Berg WAM, Boerjan M, and Müller F. Carbon-13 and nitrogen-15 nuclear magnetic resonance study on the interaction between riboflavin and riboflavin-binding apoprotein. *Biochemistry* 23: 4873–4878, 1984.
121. Moonen CTW, Vervoort J, and Müller F. Reinvestigation of the structure of oxidized and reduced flavin: Carbon-13 and nitrogen-15 nuclear magnetic resonance study. *Biochemistry* 23: 4859–4867, 1984.
122. Moonen CTW, Vervoort J, and Müller F. Carbon-13 nuclear magnetic resonance study on the dynamics of the conformation of reduced flavin. *Biochemistry* 23: 4868–4872, 1984.
123. Morales R, Charon MH, Hudry–Clergeon G, Pétillot Y, Norager S, Medina M, and Frey M. Refined X-ray structures of the oxidized, at 1.3 Å, and reduced, at 1.17 Å, [2Fe-2S] ferredoxin from the *Cyanobacterium Anabaena* PCC7119 show redox-linked conformational changes. *Biochemistry* 38: 15764–15773, 1999.
124. Morales R, Charon MH, Kachalova G, Serre L, Medina M, Gómez–Moreno C, and Frey M. A redox-dependent interaction between two electron-transfer partners involved in photosynthesis. *EMBO Rep* 1: 271–276, 2000.
125. Nagpal A, Valley MP, Fitzpatrick PF, and Orville AM. Crystal structures of nitroalkane oxidase: Insights into the reaction mechanism from a covalent complex of the flavoenzyme trapped during turnover. *Biochemistry* 45: 1138–1150, 2006.
126. Nogués I, Hervás M, Peregrina JR, Navarro JA, de la Rosa MA, Gómez–Moreno C, and Medina M. *Anabaena* flavodoxin as an electron carrier from photosystem I to ferredoxin-$NADP^+$ reductase. Role of flavodoxin residues in protein–protein interaction and electron transfer. *Biochemistry* 44, 97–104, 2005.
127. Odat O, Matta S, Khalil H, Kampranis SC, Pfau R. Tscichlis PN, and Makris AM. Old yellow enzymes, highly homologous FMN oxidoreductases with modulating roles in oxidative stress and programmed cell death in yeast. *J Biol Chem* 282: 36010–36023, 2007.
128. Okajima K, Fukushima Y, Suzuki H, Kita A, Ochiai Y, Katayama M, Shibata Y, Miki K, Noguchi T, Itoh S, and Ikeuchi M. Fate determination of the flavin photoreceptors in the cyanobacterial blue light receptor TePixD (Tll0078). *J Mol Biol* 363: 10–18, 2006.
129. Ostrovsky de Spicer P, O'Brien K, and Maloy S. Regulation of proline utilization in *Salmonella typhimurium*: A membrane-associated dehydrogenase binds DNA *in vitro*. *J Bacteriol* 173: 211–219, 1991.
130. Palmer MH, Simpson I, and Platenkamp RJ. The electronic structure of flavin derivatives: Part I. *Ab initio* calculations for 1H-alloxazine and 10H-isoalloxazine, their reduced derivatives and related compounds; Assignments of photoelectron spectra. *J Mol Struct* 66: 243–263, 1980.
131. Partch CL, Clarkson MW, Özgür S, Lee AL, and Sancar A. Role of structural plasticity in signal transduction by the cryptochrome blue-light photoreceptor. *Biochemistry* 44: 3795–3805, 2005.
132. Pawelek PD, Cheah J, Coulombe R, Macheroux P, Ghisla S, and Vrielink A. The structure of L-amino acid oxidase reveals the substrate trajectory into an enantiomerically conserved active site. *EMBO J* 19: 4204–4215, 2000.
133. Penfold RJ and Pemberton JM. Sequencing, chromosomal inactivation, and functional expression in *Escherichia coli* of *ppsR*, a gene which repress carotenoid and bacteriochlorophyll synthesis in *Rhodobacter spaeroides*. *J Bacteriol* 176: 2869–2376, 1994.
134. Phang JM. The regulatory functions of proline and pyrroline-5-carboxylic acid. *Curr Top Cell Regul* 25: 91–132, 1985.
135. Platenkamp RJ, Palmer MH, and Visser JWG. *Ab initio* molecular orbital studies of closed shell flavins. *Eur Biophys J* 14: 393–402, 1987.
136. Pollegioni L, Piubelli L, Sacchi S, Pilone MS, and Molla G. Physiological functions of D-amino acid oxidases: From yeast to humans. *Cell Mol Life Sci* 64: 1373–1394, 2007.
137. Porter AG and Urbano AG. Does apoptosis-inducing factor (AIF) have both life and death functions in cells? *Bioessays* 28: 834–843, 2006.
138. Purcell EB and Crosson S. Photoregulation in prokaryotes. *Curr Opin Microbiol* 11: 168–178, 2008.
139. Pust S, Vervoort J, Decker K, Bacher A, and Müller F. ^{13}C, ^{15}N, ^{31}P NMR studies on 6-hydroxy-L-nicotine oxidase from *Arthrobacter oxidans*. *Biochemistry* 28: 516–521, 1989.
140. Rajagopal S, Key JM, Purcell EB, Boerema DJ, and Moffat K. Purification and initial characterization of a putative blue light-regulated phosphodiesterase from *Escherichia coli*. *Photochem Photobiol*. 80: 542–547, 2004.
141. Ratzkin B and Roth J. Cluster of genes controlling proline degradation in *Salmonella typhimurium. J Bacteriol* 133: 744–754, 1978.
142. Roome PW Jr, Philley JC, and Peterson, J. Purification and properties of putidaredoxin reductase. *J Biol Chem* 258: 2593–2598, 1983.
143. Rosato E, Codd V, Mazzotta G, Piccin A, Zordan M, Costa R, and Kyriacou CP. Light-dependent interaction between *Drosophila* CRY and the clock protein PER mediated by the carboxy terminus of CRY. *Curr Biol* 11: 909–917, 2001.
144. Sagara Y, Takata Y, Miyata T, Hara T, and Horiuchi T. Cloning and sequence analysis of adrenodoxin reductase cDNA from bovine adrenal cortex. *J Biochem* 102: 1333–1336, 1987.
145. Sakai T, Kagawa T, Kasahara M, Swarts TE, Christie JM, Briggs WR, Wada M, and Okada K. *Arabidopsis* nph1 and npl1: Blue light receptors that mediate both phototropism and chloroplast relocation. *Proc Natl Acad Sci USA* 98: 6969–6974, 2001.
146. Sakai M, Takahashi H. One-electron photoreduction of flavin mononucleotide: Time-resolved resonance Raman and absorption study. *J Mol Struct* 379: 9–18, 1996.
147. Salomon M, Christie JM, Knieb E, Lempert U, and Briggs WR. Photochemical and mutational analysis of the FMN-binding domains of the plant blue light receptor, phototropin. *Biochemistry* 39: 9401–9410, 2000.
148. Salomon M, Eisenreich W, Dürr H, Schleicher E, Knleb E, Massey V, Rüdiger W, Müller F, Bacher A, and Richter G. An optomechanical transducer in the blue light receptor

phototropin from *Avena sativa*. *Proc Natl Acad Sci USA* 98: 12357–12361, 2001.
149. Sancho J. Flavodoxin: sequence, folding, binding, function and beyond. *Cell Mol Life Sci* 63: 855–864, 2006.
150. Sanner C, Macheroux P, Rüterjans H, Müller F, and Bacher A. ^{15}N- and ^{13}C-NMR investigations of glucose oxidase from *Aspergillus niger*. *Eur J Biochem* 196: 663–672, 1991.
151. Scarpulla RC and Soffer RL. Membrane-bound proline dehydrogenase from *Escherichia coli*. Solubilization, purification, and characterization. *J Biol Chem* 253: 5997–6001, 1978.
152. Schürmann P and Buchanan BB. The ferredoxin/thioredoxin system of oxygenic photosynthesis. *Antioxid Redox Signal* 10: 1235–1274, 2008.
153. Senda M, Kimura S, Kishigami S, and Senda T. Crystallization and preliminary X-ray analysis of the Rieske-type [2Fe-2S] ferredoxin component of biphenyl dioxygenase from *Pseudomonas* sp. strain KKS102. *Acta Crystallogr* F62: 590–592, 2006.
154. Senda M, Kishigami S, Kimura S, Fukuda M, Ishida T, and Senda T. Molecular mechanism of the redox-dependent interaction between NADH-dependent ferredoxin reductase and Rieske-type [2Fe-2S] ferredoxin. *J Mol Biol* 373: 382–400, 2007.
155. Senda M, Kishigami S, Kimura S, and Senda T. Crystallization and preliminary X-ray analysis of the reduced Rieske-type [2Fe-2S] ferredoxin derived from *Pseudomonas* sp. strain KKS102. *Acta Crystallogr* F63: 311–314, 2007.
156. Senda M, Kishigami S, Kimura S, and Senda T. Crystallization and preliminary X-ray analysis of the electron-transfer complex of Rieske-type [2Fe-2S] ferredoxin and NADH-dependent ferredoxin reductase derived from *Acidovorax* sp. strain KKS102. *Acta Crystallogr* F63: 520–523, 2007.
157. Senda T, Yamada T, Sakurai N, Kubota M, Nishizaki T, Masai E, Fukuda M, and Mitsuidagger Y. Crystal structure of NADH-dependent ferredoxin reductase component in biphenyl dioxygenase. *J Mol Biol* 304: 397–410, 2000.
158. Sétif P. Ferredoxin and flavodoxin reduction by photosystem I. *Biochim Biophys Acta* 1507: 161–179, 2001.
159. Sevrioukova IF. Redox-dependent structural reorganization in putidaredoxin, a vertebrate-type [2Fe-2S] ferredoxin from *Pseudomonas putida*. *J Mol Biol* 347: 607–621, 2005.
160. Sevrioukova IF, Li H, and Poulos TL. Crystal structure of putidaredoxin reductase from *Pseudomonas putida*, the final structural component of the cytochrome P450cam monooxygenase. *J Mol Biol* 336: 889–902, 2004.
161. Shalitin D, Yang H, Mockler TC, Maymon M, Guo H, Whitelam GC, and Lin C. Regulation of *Arabidopsis* cryptochrome 2 by blue-light-dependent phosphorylation. *Nature* 417, 763–767, 2002.
162. Siebold C, Berrow N, Walter TS, Harlos K, Owens RJ, Stuart DI, Terman JR, Kolodkin AL, Pasterkamp RJ, and Jones EY. High-resolution structure of the catalytic region of MICAL (molecule interacting with CasL), a multidomain flavoenzyme signaling molecule. *Proc Natl Acad Sci USA* 102: 16836–16841, 2005.
163. Strassner J, Fürholz A, Macheroux P, Amrhein N, and Schaller A. A homolog of old yellow enzyme in tomato. Spectral properties and substrate specificity of the recombinant protein. *J Biol Chem* 274: 35067–35073, 1999.
164. Susin SA, Lorenzo HK, Zamzami N, Marzo I, Snow BE, Brothers GM, Mangion J, Jacotot E, Costantini P, Loeffler M, Larochette N, Goodlett DR, Aebersold R, Siderovski DP, Penninger JM, and Kroemer G. Molecular characterization of mitochondrial apoptosis-inducing factor. *Nature* 397: 441–446, 1999.
165. Swartz TE, Corchnoy SB, Christie JM, Lewis JW, Szundi I, Briggs WR, and Bogomolni RA. The photocycle of a flavin-binding domain of the blue light photoreceptor phototropin. *J Biol Chem* 39: 36493–36500, 2001.
166. Tanaka H, Yamamoto A, Ishida T, and Horiike K. D-Serine dehydratase from chicken kidney: A vertebral homologue of the cryptic enzyme from *Burkholderia cepacia*. *J Biochem* 143: 49–57, 2008.
167. Taylor BL and Zhulin IB. PAS domains: Internal sensors of oxygen, redox potential, and light. *Microbiol Mol Biol Rev* 63: 479–506, 1999.
168. Tegoni M and Cambillau C. The 2.6 Å refined structure of the *Escherichia coli* recombinant *Saccharomyces serevisiae* flavocytochrome b_2-sufite complex. *Protein Sci* 3: 303–313, 1994.
169. Theorell H. Purification of the active group of the yellow enzyme. *Biochem Z* 275: 344–346, 1935.
170. Thresher RJ, Vitaterna MH, Miyamoto Y, Kazantsev A, Hsu DS, Petit C, Selby CP, Dawut L, Smithies O, Takahashi JS, and Sancar A. Role of mouse cryptochrome blue-light photoreceptor in circadian photoresponses. *Science* 282: 1490–1494, 1998.
171. Trus BL, Wells JL, Johnstone RM, Fritsche CJ Jr, and Marsh RE. Crystal structure of the yellow 1:2 molecular complex lumiflavin-bisnaphthalene-2,3-diol. *J Chem Soc D Chem Commun* 14: 751–752, 1971.
172. Unno M, Sano R, Masuda S, Ono T, and Yamauchi S. Light-induced structural changes in the active site of the BLUF domain in AppA by Raman spectroscopy. *J Phys Chem* 109: 12620–12626, 2005.
173. van den Hemel D, Brigé A, Savvides SN, and Beeumen JV. Ligand-induced conformational changes in the capping subdomain of a bacterial old yellow enzyme homologue and conserved sequence fingerprints provide new insights into substrate binding. *J Biol Chem* 281: 28512–28161, 2006.
174. van der Horst GTJ, Muijtjens M, Kobayashi K, Takano R, Kanno S, Takao M, de Wit J, Verkerk A, Eker APM, van Leenen D, Buijs R, Bootsma D, Hoeijmakers JHJ, and Yasui A. Mammalian Cry1 and Cry2 are essential for maintenance of circadian rhythms. *Nature* 398: 627–630, 1999.
175. Vervoort J, Müller F, LeGall J, Bacher A, and Sedlmaier H. Carbon-13 and nitrogen-15 nuclear-magnetic-resonance investigation on *Desulfovibrio vulgaris* flavodoxin. *Eur J Biochem* 151: 49–57, 1985.
176. Vervoort J, Müller F, Mayhew SG, van den Berg WAM, Moonen CTW, and Bacher A. A comparative carbon-13, nitrogen-15, and phosphorus-31 nuclear magnetic resonance study on the flavodoxins from *Clostridium MP*, *Megasphaera elsdenii*, and *Azotobacter vinelandii*. *Biochemistry* 25: 6789–6799, 1986.
177. Vervoort J, van Berkel WJH, Mayhew SG, Müller F, Bacher A, Nielsen P, and LeGall J. Properties of the complexes of riboflavin 3′,5′-bisphosphate and the apoflavodoxins from *Megasphaera elsdenii* and *Desulfovibrio vulgaris*. *Eur J Biochem* 161: 749–756, 1986.
178. Vervoort J, van Berkel WJH, Müller F, and Moonen CTW. NMR studies on *p*-hydroxybenzoate hydroxylase from *Pseudomonas fluorescens* and salicylate hydroxylase from *Pseudomonas putida*. *Eur J Biochem* 200: 731–738, 1991.
179. Wang H, Ma L-G, Li J-M, Zhao H-Y, and Deng XW. Direct interaction of *Arabidopsis* cryptochromes with COP1 in light control development. *Science* 294: 154–158, 2001.

180. Wang J, Ortiz-Maldonado M, Entsch B, Massey V, Ballou D, and Gatti DL. Protein and ligand dynamics in 4-hydroxybenzoate hydroxylase. *Proc Natl Acad Sci USA* 99: 608–613, 2002.
181. Warburg O and Christian W. Ein zweites sauerstoffübertragendes Ferment und sein Absorptionspektrum. *Naturwissenschaften* 20: 688, 1932.
182. Warburg O and Christian W. Isolierung der prostethischen Gruppe der D-Aminosäure Oxydase. *Biochem Z* 298: 150–155, 1938.
183. Watenpaugh KD, Sieker LC, Jensen LH, Legall J, and Dubourdieu M. Structure of the oxidized form of a flavodoxin at 2.5-Å resolution: Resolution of the phase ambiguity by anomalous scattering. *Proc Natl Acad Sci USA* 69: 3185–3188, 1972.
184. Watt W, Tulinsky A, Swenson RP, and Watenpaugh KD. Comparison of the crystal structures of a flavodoxin in its three oxidation states at cryogenic temperatures. *J Mol Biol* 218: 195–208, 1991.
185. Werner PE and Rönnquist O. Studies on flavin derivatives. The crystal structure of 5-acetyl-9-bromo-1,3,7,8,10-pentamethyl-1,5-dihydroisoalloxazine. *Acta Chem Scand* 24: 997–1009, 1970.
186. Williams RE and Bruce N. 'New uses for an old enzyme'—the old yellow enzyme family of flavoenzymes. *Microbiology* 148: 1607–1614, 2002.
187. Wood JM. Membrane association of proline dehydrogenase in *Escherichia coli* is redox dependent. *Proc Natl Acad Sci USA* 84: 373–377, 1987.
188. Yang H-Q, Tang R-H, and Cashmore AR. The signaling mechanism of *Arabidopsis* CRY1 involves direct interaction with COP1. *Plant Cell* 13: 2573–2587, 2001.
189. Yang H-Q, Wu Y-J, Tang R-H, Liu D, Liu Y, and Cashmore AR. The C termini of *Arabidopsis* cryptochromes mediate a constitutive light response. *Cell* 103: 815–827, 2000.
190. Ye H, Cande C, Stephanou NC, Jiang S, Gurbuxani S, Larochette N, Daugas E, Garrido C, Kroemer G, and Wu H. DNA binding is required for the apoptogenic action of apoptosis inducing factor. *Nat Struct Biol* 9: 680–684, 2002.
191. Yuan H, Anderson S, Masuda S, Dragnea V, Moffat K, and Bauer C. Crystal structure of the *Synechocystis* photoreceptor Slr1694 reveal distinct structural states related to signaling. *Biochemistry* 45: 12687–12694, 2006.
192. Zhang W, Zhang M, Zhu W, Zhou Y, Wanduragala S, Rewinkel D, Tanner JJ, and Becker DF. Redox-induced changes in flavin structure and roles of flavin N(5) and the ribityl 2′-OH group in regulating PutA-membrane binding. *Biochemistry* 46: 483–491, 2007.
193. Zheng Y-J and Ornstein RL. A theoretical study of the structures of flavin in different oxidation and protonation states. *J Am Chem Soc* 118: 9402–9408, 1996.
194. Zhu W and Becker DF. Flavin redox state triggers conformational changes in the PutA protein from *Escherichia coli*. *Biochemistry* 42: 5469–5477, 2003.
195. Zhulin IB and Taylor BL. PAS domain S-boxes in archaea, bacteria and sensors for oxygen and redox. *Trends Biochem Sci* 22: 331–333, 1997.
196. Ziegler GA, Vonrhein C, Hanukoglu I, and Schulz GE. The structure of adrenodoxin reductase of mitochondrial P450 systems: Electron transfer for steroid biosynthesis. *J Mol Biol* 289: 981–990, 1999.
197. Zoltowski BD and Crane BR. Light activation of the LOV protein Vivid generates a rapidly exchanging dimer. *Biochemistry* 47: 7012–7019, 2008.
198. Zoltowski BD, Schwerdtfeger C, Widom J, Loros JJ, Bilwes AM, Dunlap JC, and Crane BR. Conformational switching in the fungal light sensor Vivid. *Science* 316: 1054–1057, 2007.

Address reprint requests to:
Toshiya Senda
Biomedicinal Information Research Center (BIRC)
National Institute of Advanced Industrial Science and Technology (AIST)
2-42 Aomi, Koto-ku
Tokyo 135-0064, Japan

E-mail: toshiya-senda@aist.go.jp

Date of first submission to ARS Central, October 25, 2008; date of final revised submission, February 15, 2009; date of acceptance, February 21, 2009.

This article has been cited by:

1. Matthew B. McNeil, Peter C. Fineran. 2012. Prokaryotic assembly factors for the attachment of flavin to complex II. *Biochimica et Biophysica Acta (BBA) - Bioenergetics* . [CrossRef]
2. Lin Z. Li. 2012. Imaging mitochondrial redox potential and its possible link to tumor metastatic potential. *Journal of Bioenergetics and Biomembranes* . [CrossRef]
3. Brian D. Zoltowski, Anand T. Vaidya, Deniz Top, Joanne Widom, Michael W. Young, Brian R. Crane. 2011. Structure of full-length Drosophila cryptochrome. *Nature* . [CrossRef]
4. Daisuke Sasaki, Masahiro Fujihashi, Yuki Iwata, Motomichi Murakami, Tohru Yoshimura, Hisashi Hemmi, Kunio Miki. 2011. Structure and Mutation Analysis of Archaeal Geranylgeranyl Reductase. *Journal of Molecular Biology* **409**:4, 543-557. [CrossRef]
5. N. Ozturk, C. P. Selby, Y. Annayev, D. Zhong, A. Sancar. 2011. Reaction mechanism of Drosophila cryptochrome. *Proceedings of the National Academy of Sciences* **108**:2, 516-521. [CrossRef]
6. Sara Ayuso-Tejedor, Vladimir Espinosa Angarica, Marta Bueno, Luis A. Campos, Olga Abián, Pau Bernadó, Javier Sancho, M. Angeles Jiménez. 2010. Design and Structure of an Equilibrium Protein Folding Intermediate: A Hint into Dynamical Regions of Proteins. *Journal of Molecular Biology* **400**:4, 922-934. [CrossRef]
7. Andreas Möglich, Xiaojing Yang, Rebecca A. Ayers, Keith Moffat. 2010. Structure and Function of Plant Photoreceptors. *Annual Review of Plant Biology* **61**:1, 21-47. [CrossRef]
8. Åsmund Kjendseth Røhr, Hans-Petter Hersleth, K. Kristoffer Andersson. 2010. Tracking Flavin Conformations in Protein Crystal Structures with Raman Spectroscopy and QM/MM Calculations. *Angewandte Chemie* NA-NA. [CrossRef]
9. Åsmund Kjendseth Røhr, Hans-Petter Hersleth, K. Kristoffer Andersson. 2010. Tracking Flavin Conformations in Protein Crystal Structures with Raman Spectroscopy and QM/MM Calculations. *Angewandte Chemie International Edition* NA-NA. [CrossRef]